Distinct pathways leading to TDP-43-induced cellular dysfunctions

Makiko Yamashita[1], Takashi Nonaka[1],*, Shinobu Hirai[2], Akiko Miwa[2], Haruo Okado[2], Tetsuaki Arai[4], Masato Hosokawa[3], Haruhiko Akiyama[3] and Masato Hasegawa[1],*

[1]Department of Neuropathology and Cell Biology, [2]Department of Brain Development and Neural Regeneration and [3]Dementia Research Project, Tokyo Metropolitan Institute of Medical Science, Tokyo 156-8506, Japan and [4]Department of Neuropsychiatry, Division of Clinical Medicine, Faculty of Medicine, University of Tsukuba, Tsukuba, Ibaraki 305-8575, Japan

TAR DNA-binding protein of 43 kDa (TDP-43) is the major component protein of inclusions found in brains of patients with amyotrophic lateral sclerosis (ALS) and frontotemporal lobar degeneration (FTLD-TDP). However, the molecular mechanisms by which TDP-43 causes neuronal dysfunction and death remain unknown. Here, we report distinct cytotoxic effects of full-length TDP-43 (FL-TDP) and its C-terminal fragment (CTF) in SH-SY5Y cells. When FL-TDP was overexpressed in the cells using a lentiviral system, exogenous TDP-43, like endogenous TDP-43, was expressed mainly in nuclei of cells without any intracellular inclusions. However, these cells showed striking cell death, caspase activation and growth arrest at G2/M phase, indicating that even simple overexpression of TDP-43 induces cellular dysfunctions leading to apoptosis. On the other hand, cells expressing TDP-43 CTF showed cytoplasmic aggregates but without significant cell death, compared with cells expressing FL-TDP. Confocal microscopic analyses revealed that RNA polymerase II (RNA pol II) and several transcription factors, such as specificity protein 1 and cAMP-response-element-binding protein, were co-localized with the aggregates of TDP-43 CTF, suggesting that sequestration of these factors into TDP-43 aggregates caused transcriptional dysregulation. Indeed, accumulation of RNA pol II at TDP-43 inclusions was detected in brains of patients with FTLD-TDP. Furthermore, apoptosis was not observed in affected neurons of FTLD-TDP brains containing phosphorylated and aggregated TDP-43 pathology. Our results suggest that different pathways of TDP-43-induced cellular dysfunction may contribute to the degeneration cascades involved in the onset of ALS and FTLD-TDP.

INTRODUCTION

TAR DNA-binding protein of 43 kDa (TDP-43) has been identified as a major component protein of the ubiquitinated inclusions characteristic of amyotrophic lateral sclerosis (ALS) and frontotemporal lobar degeneration with ubiquitin-positive inclusions (FTLD-U or FTLD-TDP) (1,2). TDP-43 is a ubiquitously expressed nuclear protein and is implicated in exon splicing, gene transcription, regulation of mRNA stability and biosynthesis and formation of nuclear bodies (3–7). It is a 414-amino acid protein with two highly conserved RNA recognition motifs (RRM1 and RRM2) and a glycine-rich region

mediating protein–protein interactions at the C-terminus (8–11). In TDP-43 proteinopathy, pathological TDP-43 is abnormally phosphorylated, ubiquitinated and N-terminally cleaved to generate C-terminal fragments (CTFs) (1,12,13).

As autosomal-dominant missense mutations in the *TARDBP* gene were identified in patients with ALS or FTLD-TDP, toxic gain of function of TDP-43 may be related to neuronal degeneration. However, in most cases of TDP-43 proteinopathy, no *TARDBP* mutations are identified, suggesting that wild-type TDP-43 itself is central to the disease cascade. A 2-fold increase in total *TARDBP* mRNA was reported in a 3′-untranslated region variant carrier (14), which suggests that just an increased level of

---

*To whom correspondence should be addressed at: Department of Neuropathology and Cell Biology, Tokyo Metropolitan Institute of Medical Science, 2-1-6, Kamikitazawa, Setagaya-ku, Tokyo 156-8506, Japan. Tel: +81 36834 2349; Fax: +81 36834 2349; Email: nonaka-tk@igakuken.or.jp (T.N.), hasegawa-ms@igakuken.or.jp (M.H.)

TDP-43 protein (22%) can cause FTLD-TDP. Similarly, overexpression of wild-type TDP-43 causes motor neuron degeneration in yeast, mice and rats (15–17). Moreover, it has recently been reported that the C-terminal portion of TDP-43 shows sequence similarity to prion protein (18) and that truncated CTFs of TDP-43 readily form intracellular aggregates in cultured cells (19–21), suggesting that not only FL-TDP but also its CTFs contribute to the pathogenesis of TDP-43 proteinopathy. However, the molecular mechanisms through which FL-TDP or aggregated CTFs cause neuronal dysfunctions leading to cell death remain unknown. To identify the mechanisms involved, we examined whether overexpression of FL-TDP or its CTF induced cell death in human neuroblastoma line SH-SY5Y cells. We report here that two different pathways lead to cellular dysfunctions induced by FL-TDP and by its CTF. We observed striking apoptotic cell death and cell cycle arrest at the G2/M phase in cells overexpressing FL-TDP. In cells overexpressing TDP-43 CTF, RNA polymerase II (RNA pol II) and several transcription factors such as specificity protein 1 (Sp1) and cAMP-response-element-binding protein (CREB) were co-localized with cytoplasmic aggregates of TDP-43 CTF and their transcriptional activities were decreased, although apoptotic cell death was not significant. These results suggest that recruitment of these factors may cause transcriptional dysregulation, thereby leading to cellular dysfunctions. Dysregulation of FL-TDP expression and/or cytoplasmic accumulation of TDP-43 CTF may contribute to the pathogenesis of ALS and FTLD-TDP.

RESULTS

Overexpression of FL-TDP or its CTF causes cellular dysfunctions in SH-SY5Y cells

Gitcho *et al.* (14) reported a 2-fold increase in total expression of *TARDBP* in a 3′-untranslated region variant carrier of FTLD-TDP, and mice or yeasts overexpressing human TDP-43 develop various abnormalities, including cytotoxicity, neuronal loss and motor deficits (15,17). These findings suggest that overexpression of TDP-43 can cause neuronal degeneration *in vivo*. However, no striking cell death was detected in cultured SH-SY5Y cells transiently expressing a plasmid encoding FL-TDP (20,22). Therefore, to examine whether more substantial and stable expression of TDP-43 is required for induction of its cytotoxic effect in cultured cells, we used a lentiviral system for expression of TDP-43. We prepared SH-SY5Y cells stably expressing FL-TDP (FL-TDP), a deletion mutant of the nuclear localization signal [ΔNLS-TDP; 78–84 residues (23)] and CTF of TDP-43 [C-TDP; 162–414 residues (20)], by using a lentiviral expression system (Fig. 1A). At 3 days after infection, transfected cells were subjected to immuno-histochemical and biochemical analyses. Confocal microscopic analyses (Fig. 1B) showed that FL-TDP was expressed mainly in nuclei, but was not phosphorylated or aggregated. ΔNLS-TDP was expressed mainly in cytoplasm, without phosphorylation or aggregation. In cells expressing C-TDP, phosphorylated and aggregated C-TDP was detected with phospho-TDP-43 specific antibody, anti-pS409/410 (Fig. 1B). Immunoblot analyses of transfected cell lysates also revealed that FL-TDP and ΔNLS-TDP were recovered mainly in Triton X-100 (TX)-sup fraction without phosphorylation, while C-TDP was phosphorylated and aggregated in TX-ppt fraction, as shown in Figure 1C.

We examined the cytotoxic effects of these TDP-43 constructs in SH-SY5Y cells. At 4 days after lentiviral infection, the viability of cells transfected with FL-TDP was strongly suppressed and striking cell death was observed (Fig. 2A–C), suggesting that expression of FL-TDP is highly cytotoxic for SH-SY5Y cells. As shown in Figure 2D, poly(ADP-ribose) polymerase (PARP), a well-known substrate for activated caspase-3, was cleaved in cells expressing FL-TDP. This result clearly indicates that expression of FL-TDP induces apoptotic cell death. On the other hand, expression of ΔNLS-TDP or C-TDP did not influence the viability at 4–7 days (Fig. 2B). We also found that expression of the N-terminal fragment of TDP-43 (N-TDP: 1–161 residues) has no cytotoxic effect (Supplementary Material, Fig. S1). In cells expressing C-TDP, however, the number of living cells was significantly less than that in mock cells or cells expressing ΔNLS-TDP at 7 days (Fig. 2C). These results suggest that expression of not only FL-TDP but also CTF of TDP-43 causes cellular dysfunctions in SH-SY5Y cells, and may indicate that expression of FL-TDP without aggregate formation and expression of CTF with inclusions induce cellular damage through distinct mechanisms.

Different modes by which FL-TDP and its CTF induce cellular dysfunctions

To examine this possibility, we performed BrdU incorporation assay in cells expressing green fluorescent protein (GFP)-tagged FL-TDP (GFP-FL-TDP) or CTF (GFP-C-TDP) (Fig. 3A). Since stable expression of TDP-43 using the lentiviral system often resulted in severe damage to SH-SY5Y cells, we mainly used cells transiently expressing TDP-43 plasmids in subsequent work. SH-SY5Y cells were transfected with a plasmid encoding GFP-FL-TDP or GFP-C-TDP for 3 days, then treated with BrdU. After 10 h incubation, the cells were fixed and stained with anti-BrdU antibody and observed with a confocal microscope. As shown in Figure 3B and C, incorporation of BrdU in cells expressing GFP-FL-TDP was significantly decreased when compared with that in cells expressing the empty vector (pEGFP), indicating that DNA synthesis and cell growth were suppressed by overexpression of GFP-FL-TDP. We also found that cells with diffuse expression of GFP-C-TDP were stained with anti-BrdU antibody, while cells including GFP-C-TDP aggregates were not (Fig. 3B, right). Quantitative analysis showed that BrdU incorporation was almost wholly suppressed in cells with GFP-C-TDP inclusions (Fig. 3C). These results indicate that suppression of cell growth owing to formation of GFP-C-TDP inclusions is more marked than that owing to expression of GFP-FL-TDP or GFP-C-TDP without inclusions.

Next, we analyzed the cell cycle by measuring the DNA content of propidium iodide (PI)-stained cells. SH-SY5Y cells were transfected with GFP-FL-TDP or GFP-C-TDP. Three days after transfection, cells were stained with PI and analyzed using a flow cytometer. As shown in Figure 4A and B, cells transfected with GFP-FL-TDP were extensively accumulated in the G2/M and subG1 phases when compared with those transfected with empty vector (pEGFP) or GFP-C-TDP. It is well known that apoptotic cells are accumulated in the subG1 phase, and an increase of cells in the G2/M phase reflects growth arrest, leading to apoptosis. This result shows that overexpression of GFP-FL-TDP induces apoptosis, which is consistent with the
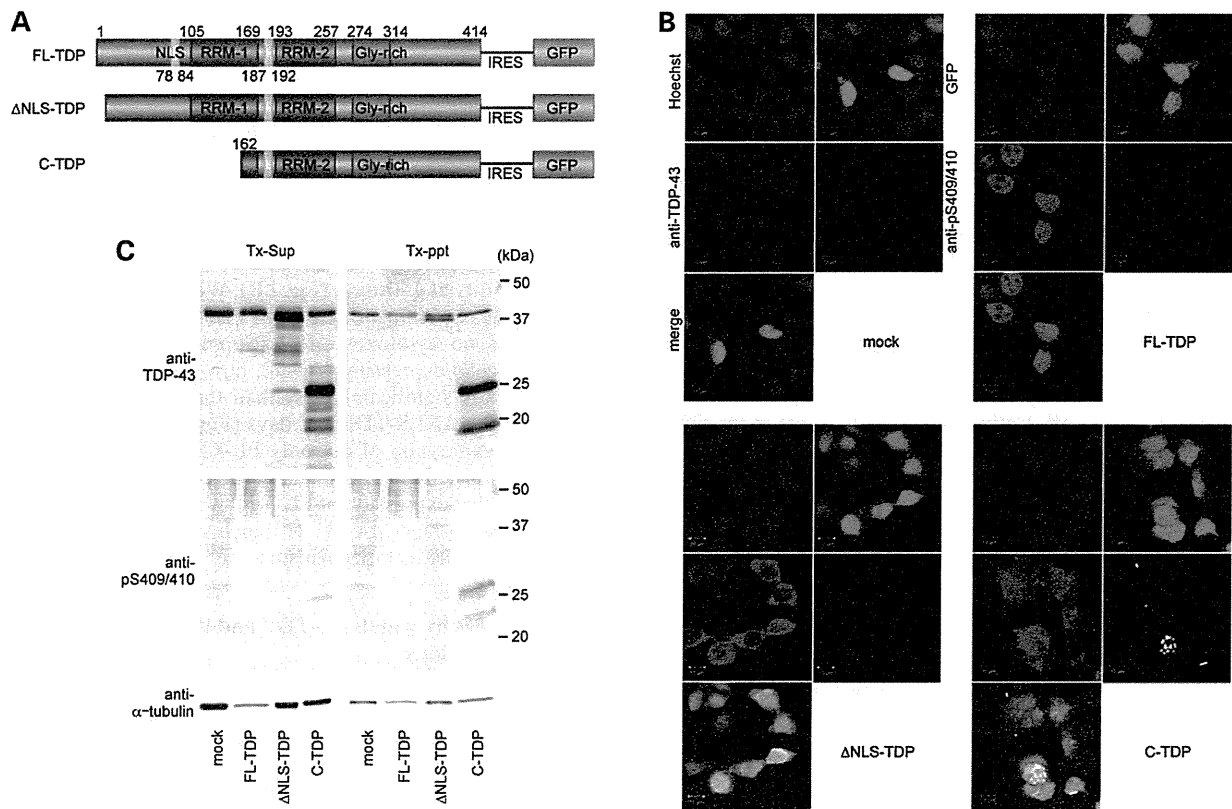
Figure 1. Overexpression of TDP-43 constructs in SH-SY5Y cells. (**A**) Schematic representation of FL-TDP, TDP-43 with deletion of the nuclear localization signal [78–84 residues (23)] (ΔNLS-TDP) and CTF (C-TDP) constructs in lentiviral expression system. RNA recognition motifs (RRM-1 and RRM-2: blue) and glycine-rich domain (Gly-rich: red) are shown. (**B**) SH-SY5Y cells were infected with each TDP-43 virus at 2×10^7 copies/well. At 4 days after infection, the cells were fixed and stained with anti-TDP-43 and anti-phospho-TDP-43 (anti-pS409/410) antibodies. Scale bars, 10 μm. (**C**) Transfected cells were also prepared for western blotting (20, 22). Cell lysates were extracted with 1% Triton X-100 (Tx), and the supernatants (Tx-sup) and insoluble pellets (Tx-ppt) after centrifugation at 100 000g for 20 min were analyzed by immunoblotting. The blots were probed with anti-TDP-43, anti-pS409/410 or anti-tubulin antibody.

result obtained in the case of lentiviral expression of FL-TDP (Fig. 2D). On the other hand, the cell cycle distribution of cells expressing GFP-C-TDP was not changed when compared with that of cells transfected with pEGFP empty vector, indicating that apoptosis is not induced in cells with formation of GFP-C-TDP aggregates. Taking these results together, it appears that overexpression of GFP-FL-TDP caused mild suppression of DNA synthesis and striking induction of apoptosis, whereas significant suppression of DNA synthesis and no abnormalities in the cell cycle were seen in cells including GFP-C-TDP aggregates. These results clearly indicate that cell death is induced via distinct molecular pathways upon overexpression of different TDP-43 species.

RNA pol II and some transcription factors are co-localized with TDP-43 inclusions and their activities are suppressed

It has been reported that transcriptional dysregulation is one of the central pathogenic mechanisms in Alzheimer's disease, Parkinson's disease and Huntington's disease (24). A number of transcriptional regulators, such as Sp1 and CREB, interact with protein aggregates, resulting in functional disruption of

these transcriptional factors in brain, followed by neurodegeneration (25–27). Therefore, to check whether these transcriptional factors are also associated with aggregates of TDP-43 CTF, we examined the localization of these factors as well as RNA pol II, which is a major enzyme responsible for transcription of protein-encoding genes. SH-SY5Y cells were transfected with GFP-C-TDP and incubated for 3 days, followed by immunohistochemical analyses. As shown in Figure 5A, inclusions composed of GFP-C-TDP were found to be positive for anti-RNA pol II antibody in cells expressing GFP-C-TDP. Furthermore, endogenous Sp1 and CREB were also co-localized with these inclusions. This result clearly shows that not only endogenous RNA pol II but also Sp1 and CREB are recruited to aggregated GFP-C-TDP. Next, we tried to confirm that endogenous RNA pol II interacts with TDP-43 biochemically. Cells expressing GFP, GFP-FL-TDP, GFP-N-TDP, GFP-C-TDP or GFP-ΔNLS-TDP were lyzed in RIPA buffer and the lysates were subjected to immunoprecipitation with anti-GFP antibody-tagged Dynabeads, followed by immunoblotting using several antibodies. We found that endogenous RNA pol II bound with phosphorylated form of GFP-C-TDP to a greater extent than did GFP-FL-TDP, GFP-N-TDP and
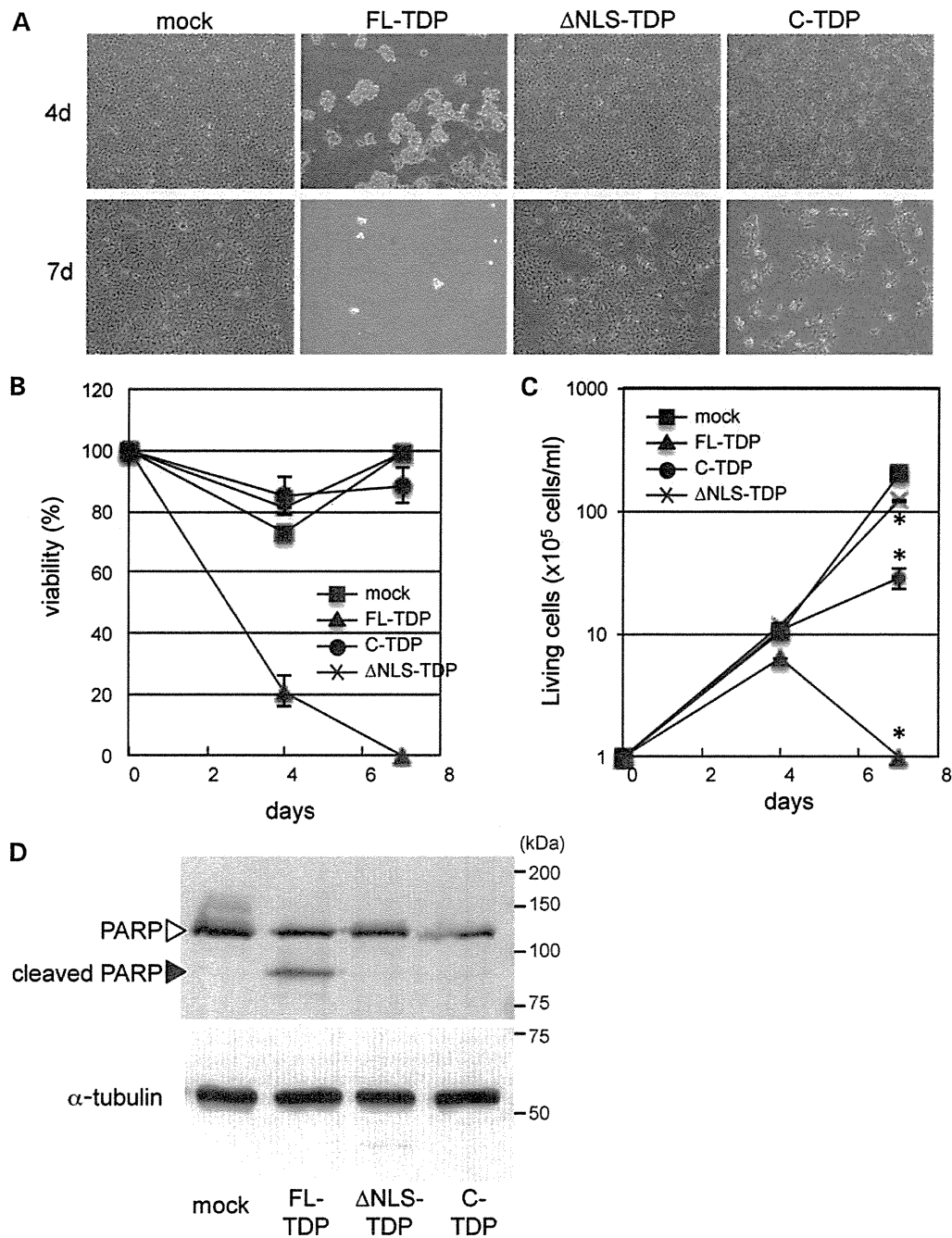
Figure 2. Cytotoxic effects of overexpressed TDP-43 in SH-SY5Y cells. SH-SY5Y cells were infected with each TDP-43 virus at 2×10^7 copies/well. At 4–7 days after infection, transfected cells were subjected to microscopic analyses, followed by cell death assay. They were assessed with light microscopy ($\times 10$ objective) at 4 and 7 days after transfection (**A**), and viability was examined by the trypan blue dye exclusion method (**B**) and living cells were counted using an automated cell counter TC10 (Bio-Rad) (**C**). The experiments were repeated three times; the illustrated results are typical. Data are means ± SEM. *$P < 0.01$ versus 'mock' by Student's *t*-test. (**D**) Transfected cells were also subjected to immunoblot analyses using anti-PARP and anti-tubulin antibodies. Note that PARP was cleaved in cells expressing FL-TDP, indicating that apoptosis is induced in these cells.

GFP-ΔNLS-TDP (Fig. 5B). We also examined the transcriptional activities of Sp1 and CREB in cells containing inclusions of GFP-C-TDP by means of luciferase assay. SH-SY5Y cells were transfected with mCherry (mC)-tagged full-length (mC-FL), ΔNLS (mC-ΔNLS) or CTF of TDP-43 (162–414 residues, mC-C), followed by co-transfection of pFR-Luc together
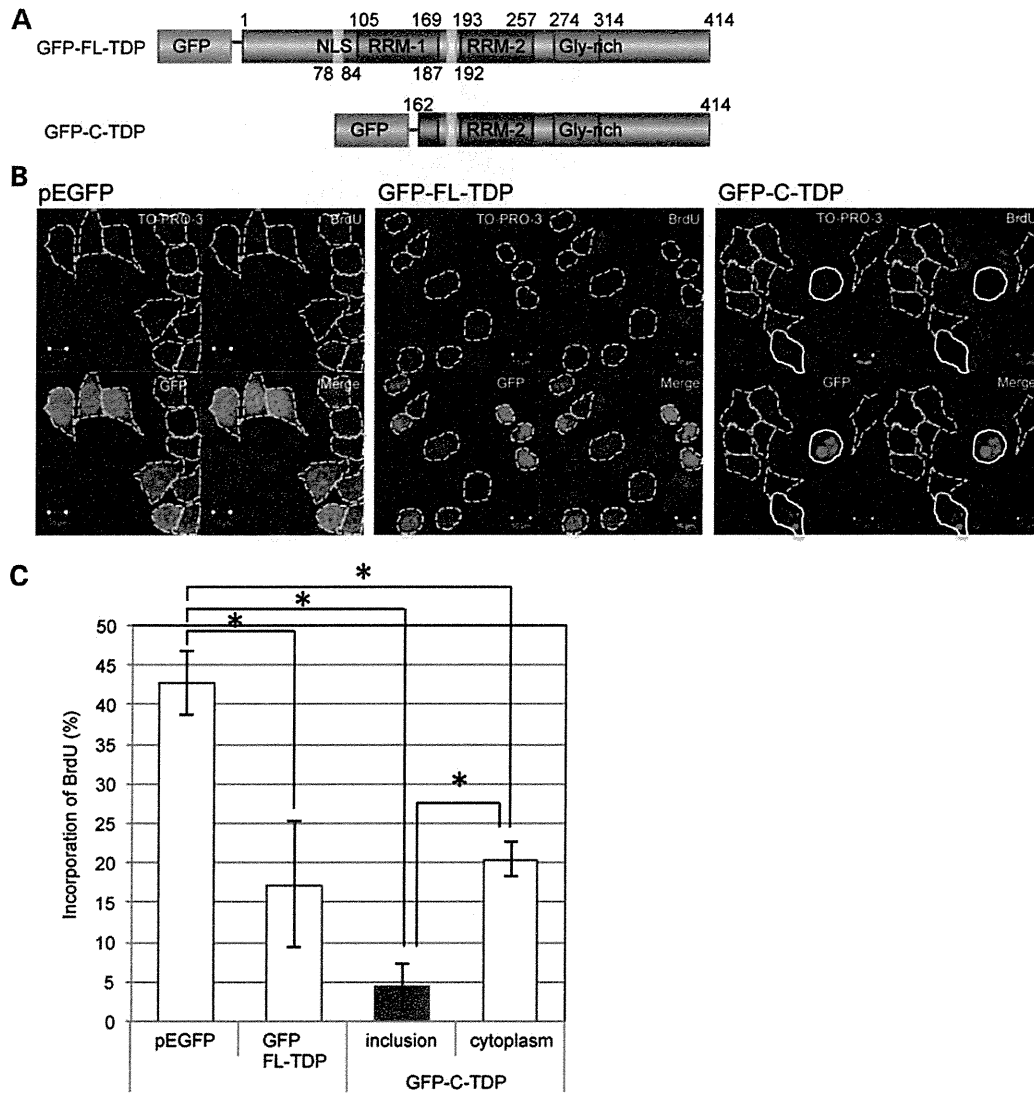
Figure 3. Comparison of cytotoxic effects of FL-TDP and its CTF. (**A**) Schematic representation of GFP-FL-TDP and GFP-C-TDP constructs in transient expression systems. (**B** and **C**) SH-SY5Y cells were transfected with the empty (pEGFP), GFP-FL-TDP or GFP-C-TDP vector for 3 days. After incubation, DNA synthesis was measured by BrdU uptake assay, using a confocal laser microscope (B). Scale bars, 10 μm. The positions of cells are indicated with broken white lines. Cells with GFP-C-TDP inclusions are indicated with white lines. The ratio (%) of the numbers of BrdU-positive cells to the numbers of GFP-positive cells was calculated as the incorporation ratio of BrdU (C). At least eight areas per sample were analyzed ($n = 8–16$), and the experiments were repeated three times; the illustrated results are typical. Data are means ± SEM. *$P < 0.01$ by Student's t-test.

with pGAL4-Sp1 or pGAL4-CREB. At 48 h after transfection, cells were harvested and the luciferase activity was measured. Figure 5C shows that the transcriptional activities of Sp1 and CREB were significantly suppressed not only in cells transfected with mC-C but also in cells expressing mC-FL. We also observed co-localization of GFP-FL-TDP with Sp1, as well as co-localization of GFP-FL-TDP with CREB (Supplementary Material, Fig. S2). However, transcriptional dysregulation caused by the expression of GFP-FL-TDP appears to be due to its high toxicity (Fig. 2B), rather than the co-localization. Alternatively, it is possible that cellular damage resulting from

overexpression of GFP-FL-TDP may cause transcriptional suppression of Sp1 and CREB.

RNA pol II co-localizes with TDP-43 inclusions in FTLD-TDP brain

To study the association of RNA pol II and transcriptional factors with TDP-43 aggregates in diseased brains, we carried out immunostaining of sporadic FTLD-TDP brain with several antibodies. As shown in Figure 6A and B, dystrophic neurites (DNs) were immunopositive for both anti-RNA pol II and
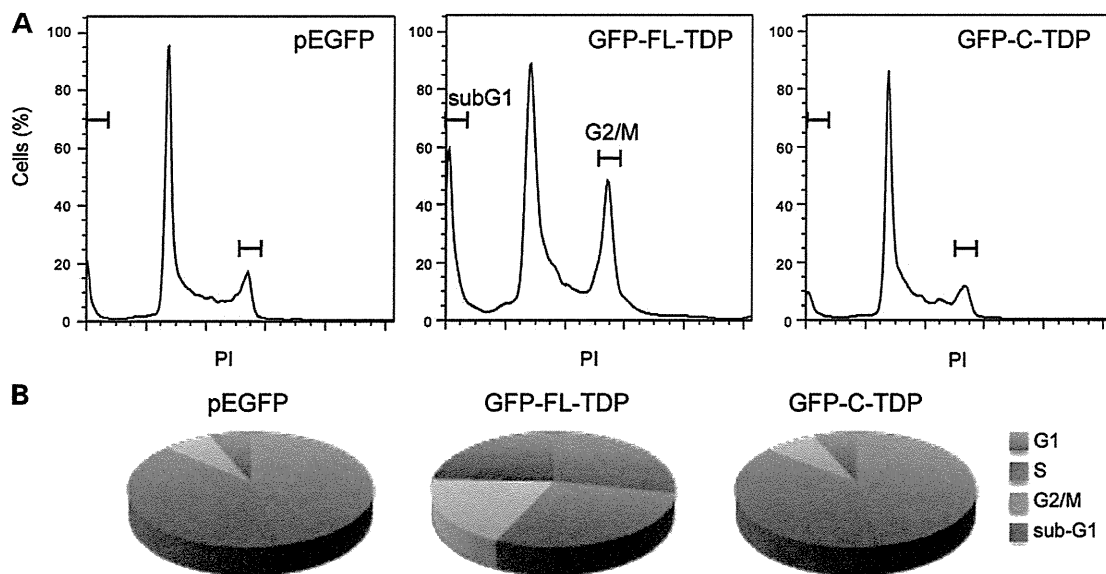
Figure 4. Analyses of the cell cycle distribution of cells transfected with GFP-tagged TDP-43. At 48 h after transfection of SH-SY5Y cells with GFP-tagged TDP-43 constructs or pEGFP empty vector, cells were stained with PI and analyzed with a flow cytometer. The results of flow-cytometric analyses are shown (**A**). The proportions of cells in G1, S, G2/M and subG1 phases were calculated using the Watson Pragmatic model (**B**). Note that growth arrest at G2/M phase was observed in GFP-FL-TDP-transfected cells, but not in GFP-C-TDP-transfected cells.

anti-pS409/410. In fluorescence-microscopic analyses, RNA pol II was co-localized with phosphorylated TDP-43 in DNs (Fig. 6D–F), clearly indicating that RNA pol II is indeed recruited to TDP-43 inclusions in FTLD-TDP brain as well as in cultured cells expressing GFP-C-TDP (Fig. 5A). On the other hand, unfortunately, antibodies to transcriptional factors Sp1, CREB and TAF II p130 failed to stain phosphorylated TDP-43 inclusions. These antibodies also failed to stain the nuclei of normal neurons in FTLD brains (data not shown). These results suggest the possibility that transcriptional activity is dysregulated *in vivo* as well as in cultured cells.

Apoptosis is not induced in FTLD-TDP brains

To test whether apoptosis is induced in FTLD-TDP brains, we performed immunoblot analyses of human brain lysates using anti-PARP and pS409/410 antibodies. As controls, we analyzed two control brains without any protein deposition and unaffected cerebellum of FTLD-TDP, in which no accumulation of TDP-43 and no atrophy has been reported. As shown in Figure 7, caspase-3-cleaved PARP was not detected in these control brains and the cerebellum of the FTLD-TDP case as well as in the temporal cortex of the FTLD-TDP case showing accumulation of TDP-43. This result indicates that apoptosis is not induced in affected neurons containing phosphorylated and aggregated TDP-43 *in vivo*.

DISCUSSION

Aberrant protein aggregates in affected neurons are well-known hallmarks of neurodegenerative diseases such as Alzheimer's disease and Parkinson's disease, but the mechanisms by which these aggregates elicit neuronal degeneration remain unclear. In TDP-43 proteinopathy, inclusion bodies composed of phosphorylated, ubiquitinated and fragmented TDP-43 were found in neuronal cells of brains or spinal cords of patients. Recently, it was reported that prion-like propagation of aggregated TDP-43 is associated with the onset and progression of TDP-43 proteinopathy (22,28). So, in order to clarify the significance of TDP-43 inclusions in disease pathogenesis, we tried to establish cellular models with stable or transient TDP-43 expression in SH-SY5Y cells.

When we overexpressed FL-TDP in SH-SY5Y cells, significant cell death, suppression of cell growth, cleavage of PARP and increased cell populations at the G2/M and sub G1 phase were detected. However, intracellular inclusions of TDP-43 were not observed in these cells. These results suggest that an abnormally increased level of TDP-43, but not its aggregates, may be necessary for induction of cellular damage leading to apoptotic cell death. Indeed, several studies reporting that endogenous TDP-43 expression is tightly regulated and is critical for survival are consistent with this idea. For example, overexpression of wild-type TDP-43 caused motor neuron degeneration in yeast and rodents (15,17), knockout of TARDBP in mice led to embryonic lethality (29–32), heterozygous knockout mice develop motor impairments with age (30), and conditional knockout mice exhibit rapid postnatal lethality (29). TDP-43 is also regulated at the mRNA level through a negative feedback loop (3). These studies indicate that cellular TDP-43 levels are under tight control and perturbation of normal TDP-43 function is detrimental. Furthermore, it was reported that wild-type human TDP-43 expression causes mitochondrial aggregation in transgenic mice (33). This result suggests the possibility that apoptotic cell death found in cells expressing FL-TDP in this study may be caused by TDP-43-induced mitochondrial dysfunction.
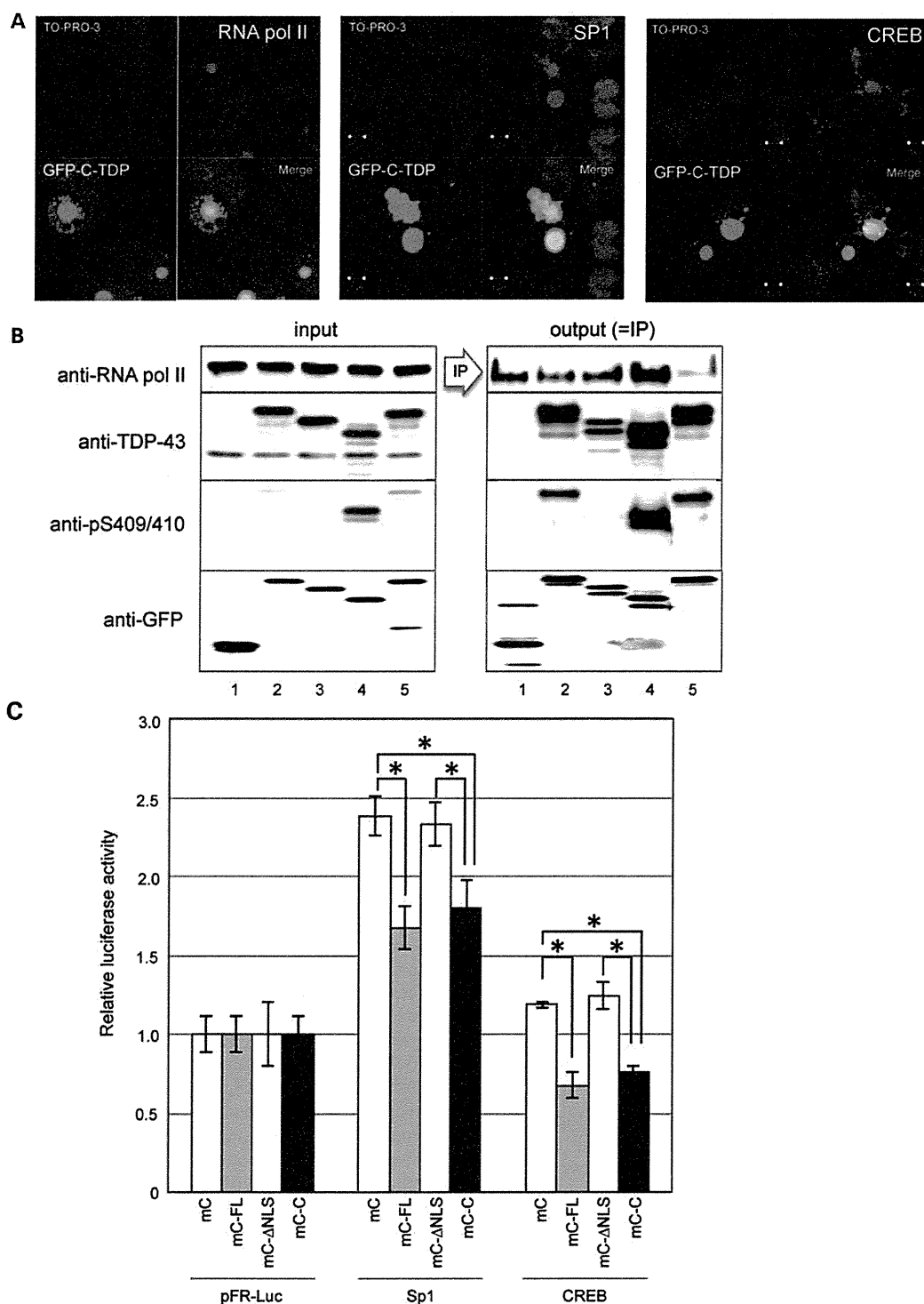
Figure 5. Co-localization of RNA pol II, Sp1 and CREB with intracellular inclusions of TDP-43 CTF. (**A**) At 72 h post-transfection with GFP-C-TDP, SH-SY5Y cells were stained with antibodies for RNA pol II, Sp1 and CREB, and observed with a confocal laser microscope. Scale bars, 5 μm. (**B**) Immunoprecipitation of cells transfected with GFP-tagged TDP-43 was performed with anti-GFP, and each sample was subjected to immunoblotting with anti-RNA pol II, TDP-43, pS409/410 and GFP antibodies. 1: pEGFP; 2: GFP-FL-TDP; 3: GFP-N-TDP (TDP-43 N-terminal fragment of 1–161 residues); 4: GFP-C-TDP and 5: GFP-ΔNLS-TDP. (**C**) SH-SY5Y cells were transfected with mCherry (mC)-tagged ΔNLS-TDP-43 (mC-ΔNLS) or CTF (mC-C). On the next day, cells were co-transfected with pFR-Luc together with pGAL4-Sp1 or pGAL4-CREB. At 48 h after the second transfection, cells were collected and luciferase activity was measured. At least three points were measured for each sample ($n = 3$–6), and the experiment was repeated three times; the illustrated results are typical. Data are means ± SEM. *$P < 0.01$ by Student's t-test.
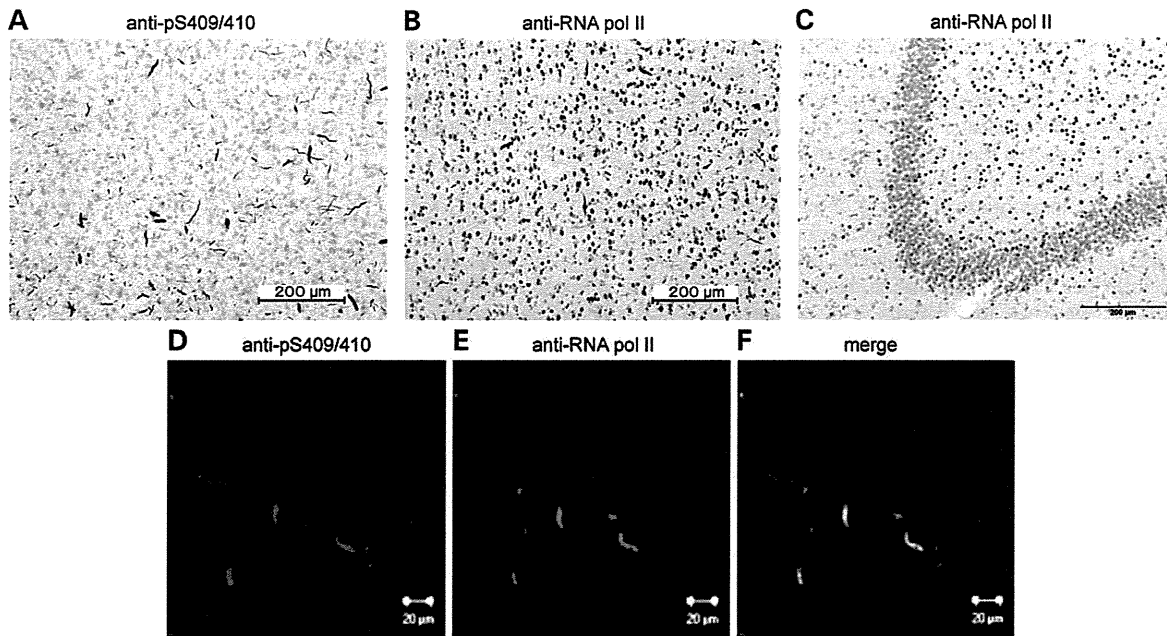
Figure 6. RNA pol II co-localizes with DNs in FTLD-TDP brain. Immunohistochemical stainings of sporadic FTLD-TDP (**A** and **B**) and control brain (**C**) were performed with anti-pS409/410 and anti-RNA pol II antibodies. (A–C) Bright-field images. Scale bars, 200 μm. (**D**–**F**) fluorescence images of sporadic FTLD-TDP. (A and D), anti-pS409/410; (B, C and E), anti-RNA pol II; (F), merge of (D) and (E). Scale bars, 20 μm.
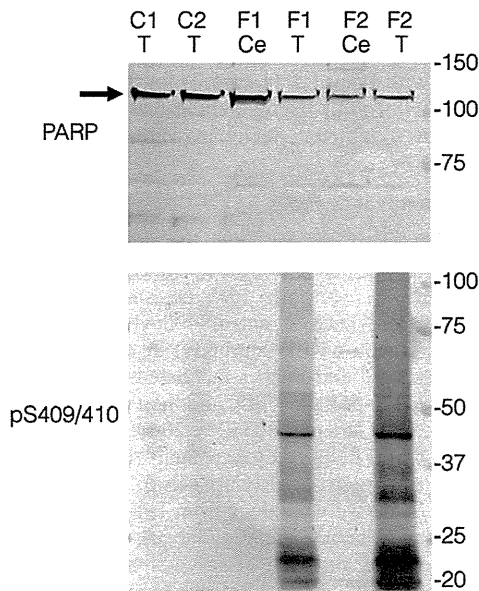

Figure 7. Apoptosis is not induced in affected neurons of FTLD-TDP brains. Immunoblot analyses of Tris-soluble (upper) and Sarkosyl-insoluble fraction (lower) prepared from human brain tissues (C1 and C2: control brains, F1 and F2: FTLD-TDP brains) were performed using anti-PARP (upper) and anti-pS409/410 (lower) antibodies. Ce, cerebellum; T, temporal cortex. Bands of endogenous whole PARP (∼120 kDa: arrow) were detected in controls and patients, but no caspase-cleaved band (∼95 kDa) was detected in affected or non-affected brains.

It remains unclear, however, how TDP-43 induces neuronal apoptotic cell death.

TDP-43 is a heterogeneous nuclear ribonucleoprotein and functions in RNA transcription and pre-mRNA splicing (34–38). In several genes, TDP-43 has been shown to bind directly to pre-mRNAs and regulate their splicing (36–42). In fact, widespread dysregulation of pre-mRNA splicing has been found in TDP-43-depleted cultured cells, TDP-43-depleted mouse brain and affected tissues from ALS patients (36–38, 41–44). These results suggest that dysregulation of pre-mRNA splicing is associated with ALS pathogenesis (38). Pre-mRNA splicing is mainly regulated by the spliceosome, which is a complex of small nuclear ribonucleoproteins (snRNPs) (38). The biogenesis of spliceosomes is regulated in Gemini of coiled bodies (GEMs) (38, 45–47). TDP-43 is likely to associate with GEMs in cultured cells (7), suggesting that TDP-43 contributes to GEM formation or function (38). Recently, it has been reported that the number of GEMs and the level of uridine-rich snRNA were decreased in spinal motor neurons of ALS patients (38, 48), suggesting that abnormal splicing caused by spliceosome disruption results in motor neuron death in ALS. Furthermore, several RNA processing genes have been shown to be mutated or genetically associated with ALS, including not only TDP-43, but also FUS/TLS, again suggesting that disordered RNA processing may be a key pathogenic mechanism in development of ALS (49). To our knowledge, the evidence presented here is the first to show that the formation of inclusions composed of TDP-43 CTF is cytotoxic: in cells with these inclusions, we observed a significant decrease of BrdU uptake, sequestration of RNA pol II, Sp1 and CREB into cytoplasmic aggregates of TDP-43 CTF, and

decreased transcriptional activities of Sp1 and CREB. Further-more, RNA pol II was co-localized with these inclusions both in cultured cells and FTLD-TDP brain. These results also support the idea that transcriptional deregulation plays a critical role in the degenerative cascade in TDP-43 proteinopathy.

Our results have shown that perturbation of the expression of FL-TDP elicits apoptotic cell death, and intracellular TDP-43 aggregation causes aberrations in RNA metabolism. The overproduction of TDP-43 might also lead to formation of intracellular TDP-43 aggregates, while decreased levels of TDP-43 protein could also influence TDP-43 expression, because TDP-43 itself auto-regulates its mRNA levels through a negative feedback loop (3). Intracellular TDP-43 aggregate formation may cause aberrant TDP-43 mRNA levels due to decreased levels of normal TDP-43 in nuclei, and this is known to be one of pathological characteristics found in brains of TDP-43 proteinopathy patients. On the other hand, lacking of apoptosis in FTLD-TDP brains containing phosphorylated and accumulated TDP-43 observed in this study suggests that non-apoptotic cytotoxicity induced by TDP-43 aggregates rather than soluble TDP-43 may be closely related to the neurodegenerative mechanisms of TDP-43 proteinopathy. Therefore, it is likely that the loss of function and the gain of toxic function of TDP-43 are mutually associated with the onset of TDP-43 proteinopathy.

We conclude that dysregulation of FL-TDP expression causes neuronal apoptosis, while formation of intracellular aggregates of TDP-43 CTF induces defects in RNA metabolism. Our results suggest that plural pathways lead to TDP-43-induced cellular dysfunction, contributing to the degeneration cascades associated with onset of TDP-43 proteinopathy.

MATERIALS AND METHODS

Antibodies

A monoclonal antibody specific for TDP-43 (anti-TDP-43) was purchased from ProteinTech. An antibody specific for phosphorylated TDP-43 at both Ser409 and Ser410 antibodies (anti-pS409/410) were prepared as described (12,50). Anti-PARP antibody (#9542) was purchased from Cell Signaling. A monoclonal anti-RNA poly II antibody, which recognizes both the phosphorylated and non-phosphorylated forms of the C-terminal heptapeptide repeat region of RNA pol II, was purchased from Active Motif. A polyclonal anti-Sp1 antibody was purchased from Bethyl Laboratories and a monoclonal anti-CREB antibody (M01) was purchased from Abnova. Anti-GFP antibody was obtained from MBL (Nagoya, Japan). Anti-tubulin α antibody was purchased from Sigma-Aldrich. Anti-mouse IgM conjugated with Alexa-568 (A-21043) and anti-rabbit IgG conjugated with Alexa-568 (A-11011) were obtained from Molecular Probes.

Viral transduction of TDP-43 constructs

FL-TDP, NTF (1–161 residues: N-TDP) and CTF [162–414 residues: C-TDP (20)] of TDP-43 were subcloned into the pCL36-C1L-CMp-IRES-GFP lentivirus expression vector (51). HEK 293T cells were transfected with vector containing the insert or the empty vector along with Packing Mix (pCAG-kGP4.1R, pCAG4-RTR2 and pCAGGS-VSV-G vectors) for

40 h (with medium replacement after 6 h). Virus particles were pelleted by ultra-centrifugation (5800*g*, Beckman SE28 rotor, 16 h, 4°C). Viruses were then suspended in Hanks Balanced Salt Solution and stored at −80°C until use. For transfection, virus (1×10^7 copies/ml) was added to 2×10^5 SH-SY5Y cells/ml.

Cell culture and transfection

SH-SY5Y cells were cultured in DMEM/F12 medium (Sigma) supplemented with 10% fetal calf serum, penicillin–streptomycin–glutamine (Invitrogen), and MEM non-essential amino acid solution (Invitrogen). The cells were maintained at 37°C under a humidified atmosphere of 5% (v/v) CO_2 in air. They were grown to 50% confluence in six-well culture dishes for transient expression, and transfected with expression plasmids using FuGENE6 (Roche) according to the manufacturer's instructions. TDP-43 expression plasmids for FL-TDP and C-TDP were constructed as previously described (20,23).

Cell proliferation assay

Cell proliferation was determined with a 5-Bromo-2′-deoxy-uridine Labeling and Detection Kit II (Roche). Transfected SH-SY5Y cells were grown on coverslips for 3 days, and then incubated for 10 h at 37°C in culture medium containing 10 μM BrdU. After incubation, cells were washed briefly, fixed and processed for immunostaining according to the manufacturer's instructions.

Cell cycle analysis

Cells were harvested at 72 h after transfection, fixed in 70% ethanol, treated with RNase A (1 mg/ml) for 30 min, and then stained with PI (50 μg/ml). DNA content was analyzed using an EPICS XL flow cytometer (Beckman Coulter).

Immunohistochemical analysis

SH-SY5Y cells were grown on coverslips and transfected as described above. After incubation for the indicated times, cells were fixed with 4% paraformaldehyde and stained with primary antibody (anti-TDP-43, anti-pS409/410, anti-RNA pol II, anti-Sp1 and/or anti-CREB antibody) at 1:1000 dilution. The cells were washed and further incubated with anti-rabbit IgG-conjugated Alexa-568 (1:1000), and then with TO-PRO-3 (1:3000, Invitrogen) or Hoechst 33342 (1:2000, Lonza) to counterstain nuclear DNA. Finally, they were analyzed using a LSM5 Pascal confocal laser microscope (Carl Zeiss).

Human brain tissues were obtained from Tokyo Metropolitan Institute of Medical Science (Tokyo, Japan). This study was approved by the local research ethics committee of Tokyo Metropolitan Institute of Medical Science (approval no. 12-3). Small blocks of human brain were dissected at autopsy or from fresh-frozen brain samples and fixed in 4% paraformaldehyde in 0.1 M phosphate buffer (pH 7.4) for 2 days. Following cryo-protection with 15% sucrose in 0.01 M phosphate-buffered saline (pH 7.4), blocks were cut on a freezing microtome at 30 μm thickness. The free-floating sections were incubated with anti-pS409/410 or anti-RNA pol II antibody for 72 h.

Following treatment with the appropriate secondary antibody, labeling was detected using the avidin-biotinylated horseradish peroxidase (HRP) complex system coupled with diaminobenzidine (DAB) reaction to yield a brown precipitate. In some sections, the DAB reaction was intensified with nickel ammonium sulfate to yield a dark purple precipitate. Moreover, the sections were incubated with secondary antibodies, labeled with FITC for anti-pS409/410 or with Rhodamine for RNA pol II and then observed under a fluorescence microscopy.

Immunoprecipitation and western blotting

SH-SY5Y cells grown in a six-well plate were transfected with GFP-tagged TDP-43 expression vectors (20). After incubation for 3 days, cells were harvested and lyzed in TX buffer [50 mM Tris-HCl (pH 7.5), 150 mM NaCl, 5 mM ethylenediaminetetraacetic acid, 5 mM ethylene glycol tetraacetic acid (EGTA), 1% TX and protease inhibitor cocktail (Roche)] by brief sonication on ice. The lysates were incubated with anti-GFP antibody-linked Dynabeads (Invitrogen) for 4 h at 4°C. The immunoprecipitated Dynabeads complexes were washed five times with TX buffer. Proteins were eluted by boiling in SDS sample buffer and then processed for western blot analysis. Each sample was separated by 12% (v/v) SDS-PAGE using Tris-glycine buffer system, and proteins were transferred onto polyvinylidene difluoride membrane (Millipore). The blots were incubated overnight with each primary antibody at room temperature, followed by incubation with HRP-conjugated secondary antibody. Signals were detected using the ECL plus Western Blotting Detection System (GE Healthcare).

Luciferase assay

In the GAL4-Sp1 expression vectors, the 147 N-terminal codons of the yeast transcription factor GAL4 containing its DNA-binding domain were fused to fragments coding for the N-terminal regions of Sp1 and CREB. The expression vectors of pGAL4-Sp1 and pGAL4-CREB, and luciferase reporter plasmid pFR-Luc were prepared as described previously (52). SH-SY5Y cells were transfected with mCherry-tagged TDP-43 constructs. Next day, these cells were co-transfected with pFR-Luc together with pGAL4-Sp1 or pGAL4-CREB. At 48 h after the second transfection, cells were collected and luciferase activity was measured with a Luciferase Assay kit (Stratagene) according to the manufacturer's instructions. At least three points of each sample were measured ($n = 3-6$), and the experiment was repeated three times; the illustrated results are typical.

Preparation of human brain homogenates

Brain samples for immunoblot analyses were prepared as previously described (12,22). Briefly, frozen brain tissue from two controls or two patients with FTLD-TDP (type C) was homogenized in 10 volumes (w/v) of homogenization buffer (HB: 10 mM Tris-HCl, pH 7.4, 0.8 M NaCl, 1 mM EGTA and 10% sucrose). Aliquots of the homogenates were ultracentrifuged at 100 000*g* for 20 min at 4°C, and the supernatant was recovered as Tris-soluble fraction for immunoblotting analyses. Remaining lysate homogenates were incubated at 37°C for 30 min in HB buffer containing 2% Sarkosyl, and centrifuged at 20 000*g* for

10 min. The supernatants were ultracentrifuged at 100 000*g* for 20 min and the resulting pellets were used as Sarkosyl-insoluble fraction for immunoblotting analyses.

Statistical analysis

All values in the figures are shown as mean $\pm$ SEM. Statistical analysis was performed using the unpaired, two-tailed Student's *t*-test. A *P* value of 0.01 or less was considered to be statistically significant.

SUPPLEMENTARY MATERIAL

Supplementary Material is available at *HMG* online.

ACKNOWLEDGEMENTS

FUNDING

REFERENCES

1. Arai, T., Hasegawa, M., Akiyama, H., Ikeda, K., Nonaka, T., Mori, H., Mann, D., Tsuchiya, K., Yoshida, M., Hashizume, Y. *et al.* (2006) TDP-43 is a component of ubiquitin-positive tau-negative inclusions in frontotemporal lobar degeneration and amyotrophic lateral sclerosis. *Biochem. Biophys. Res. Commun.*, **351**, 602–611.
2. Neumann, M., Sampathu, D.M., Kwong, L.K., Truax, A.C., Micsenyi, M.C., Chou, T.T., Bruce, J., Schuck, T., Grossman, M., Clark, C.M. *et al.* (2006) Ubiquitinated TDP-43 in frontotemporal lobar degeneration and amyotrophic lateral sclerosis. *Science*, **314**, 130–133.
3. Ayala, Y.M., De Conti, L., Avendano-Vazquez, S.E., Dhir, A., Romano, M., D'Ambrogio, A., Tollervey, J., Ule, J., Baralle, M., Buratti, E. *et al.* (2011) TDP-43 regulates its mRNA levels through a negative feedback loop. *EMBO J.*, **30**, 277–288.
4. Ayala, Y.M., Zago, P., D'Ambrogio, A., Xu, Y.F., Petrucelli, L., Buratti, E. and Baralle, F.E. (2008) Structural determinants of the cellular localization and shuttling of TDP-43. *J. Cell Sci.*, **121**, 3778–3785.
5. Buratti, E. and Baralle, F.E. (2008) Multiple roles of TDP-43 in gene expression, splicing regulation, and human disease. *Front. Biosci.*, **13**, 867–878.
6. Ou, S.H., Wu, F., Harrich, D., Garcia-Martinez, L.F. and Gaynor, R.B. (1995) Cloning and characterization of a novel cellular protein, TDP-43, that binds to human immunodeficiency virus type 1 TAR DNA sequence motifs. *J. Virol.*, **69**, 3584–3596.
7. Wang, I.F., Reddy, N.M. and Shen, C.K. (2002) Higher order arrangement of the eukaryotic nuclear bodies. *Proc. Natl. Acad. Sci. USA*, **99**, 13583–13588.
8. Ayala, Y.M., Pantano, S., D'Ambrogio, A., Buratti, E., Brindisi, A., Marchetti, C., Romano, M. and Baralle, F.E. (2005) Human, Drosophila, and *C. elegans* TDP43: nucleic acid binding properties and splicing regulatory function. *J. Mol. Biol.*, **348**, 575–588.

9. Buratti, E. and Baralle, F.E. (2001) Characterization and functional implications of the RNA binding properties of nuclear factor TDP-43, a novel splicing regulator of CFTR exon 9. *J. Biol. Chem.*, **276**, 36337–36343.

10. Buratti, E., Brindisi, A., Giombi, M., Tisminetzky, S., Ayala, Y.M. and Baralle, F.E. (2005) TDP-43 binds heterogeneous nuclear ribonucleoprotein A/B through its C-terminal tail: an important region for the inhibition of cystic fibrosis transmembrane conductance regulator exon 9 splicing. *J. Biol. Chem.*, **280**, 37572–37584.

11. Wang, I.F., Wu, L.S. and Shen, C.K. (2008) TDP-43: an emerging new player in neurodegenerative diseases. *Trends Mol. Med.*, **14**, 479–485.

12. Hasegawa, M., Arai, T., Nonaka, T., Kametani, F., Yoshida, M., Hashizume, Y., Beach, T.G., Buratti, E., Baralle, F., Morita, M. *et al.* (2008) Phosphorylated TDP-43 in frontotemporal lobar degeneration and amyotrophic lateral sclerosis. *Ann. Neurol.*, **64**, 60–70.

13. Hasegawa, M., Nonaka, T., Tsuji, H., Tamaoka, A., Yamashita, M., Kametani, F., Yoshida, M., Arai, T. and Akiyama, H. (2011) Molecular dissection of TDP-43 proteinopathies. *J. Mol. Neurosci.*, **45**, 480–485.

14. Gitcho, M.A., Bigio, E.H., Mishra, M., Johnson, N., Weintraub, S., Mesulam, M., Rademakers, R., Chakraverty, S., Cruchaga, C., Morris, J.C. *et al.* (2009) TARDBP 3′-UTR variant in autopsy-confirmed frontotemporal lobar degeneration with TDP-43 proteinopathy. *Acta Neuropathol.*, **118**, 633–645.

15. Johnson, B.S., McCaffery, J.M., Lindquist, S. and Gitler, A.D. (2008) A yeast TDP-43 proteinopathy model: exploring the molecular determinants of TDP-43 aggregation and cellular toxicity. *Proc. Natl. Acad. Sci. USA*, **105**, 6439–6444.

16. Tatom, J.B., Wang, D.B., Dayton, R.D., Skalli, O., Hutton, M.L., Dickson, D.W. and Klein, R.L. (2009) Mimicking aspects of frontotemporal lobar degeneration and Lou Gehrig's disease in rats via TDP-43 overexpression. *Mol. Ther.*, **17**, 607–613.

17. Wils, H., Kleinberger, G., Janssens, J., Pereson, S., Joris, G., Cuijt, I., Smits, V., Ceuterick-de Groote, C., Van Broeckhoven, C. and Kumar-Singh, S. (2010) TDP-43 transgenic mice develop spastic paralysis and neuronal inclusions characteristic of ALS and frontotemporal lobar degeneration. *Proc. Natl. Acad. Sci. USA*, **107**, 3858–3863.

18. Guo, W., Chen, Y., Zhou, X., Kar, A., Ray, P., Chen, X., Rao, E.J., Yang, M., Ye, H., Zhu, L. *et al.* (2011) An ALS-associated mutation affecting TDP-43 enhances protein aggregation, fibril formation and neurotoxicity. *Nat. Struct. Mol. Biol.*, **18**, 822–830.

19. Igaz, L.M., Kwong, L.K., Chen-Plotkin, A., Winton, M.J., Unger, T.L., Xu, Y., Neumann, M., Trojanowski, J.Q. and Lee, V.M. (2009) Expression of TDP-43 C-terminal fragments in vitro recapitulates pathological features of TDP-43 proteinopathies. *J. Biol. Chem.*, **284**, 8516–8524.

20. Nonaka, T., Kametani, F., Arai, T., Akiyama, H. and Hasegawa, M. (2009) Truncation and pathogenic mutations facilitate the formation of intracellular aggregates of TDP-43. *Hum. Mol. Genet.*, **18**, 3353–3364.

21. Zhang, Y.J., Xu, Y.F., Cook, C., Gendron, T.F., Roettges, P., Link, C.D., Lin, W.L., Tong, J., Castanedes-Casey, M., Ash, P. *et al.* (2009) Aberrant cleavage of TDP-43 enhances aggregation and cellular toxicity. *Proc. Natl. Acad. Sci. USA*, **106**, 7607–7612.

22. Nonaka, T., Masuda-Suzukawa, M., Arai, T., Hasegawa, Y., Akatsu, H., Obi, T., Yoshida, M., Murayama, S., Mann, D.M., Akiyama, H. *et al.* (2013) Prion-like properties of pathological TDP-43 aggregates from diseased brains. *Cell Rep.*, **4**, 124–134.

23. Nonaka, T., Arai, T., Buratti, E., Baralle, F.E., Akiyama, H. and Hasegawa, M. (2009) Phosphorylated and ubiquitinated TDP-43 pathological inclusions in ALS and FTLD-U are recapitulated in SH-SY5Y cells. *FEBS Lett.*, **583**, 394–400.

24. Okazawa, H. (2003) Polyglutamine diseases: a transcription disorder? *Cell Mol. Life Sci.*, **60**, 1427–1439.

25. Sugars, K.L. and Rubinsztein, D.C. (2003) Transcriptional abnormalities in Huntington disease. *Trends Genet.*, **19**, 233–238.

26. Dunah, A.W., Jeong, H., Griffin, A., Kim, Y.M., Standaert, D.G., Hersch, S.M., Mouradian, M.M., Young, A.B., Tanese, N. and Krainc, D. (2002) Sp1 and TAFII130 transcriptional activity disrupted in early Huntington's disease. *Science*, **296**, 2238–2243.

27. Mantamadiotis, T., Lemberger, T., Bleckmann, S.C., Kern, H., Kretz, O., Martin Villalba, A., Tronche, F., Kellendonk, C., Gau, D., Kapfhammer, J. *et al.* (2002) Disruption of CREB function in brain leads to neurodegeneration. *Nat. Genet.*, **31**, 47–54.

28. Furukawa, Y., Kaneko, K., Watanabe, S., Yamanaka, K. and Nukina, N. (2011) A seeding reaction recapitulates intracellular formation of Sarkosyl-insoluble transactivation response element (TAR) DNA-binding protein-43 inclusions. *J. Biol. Chem.*, **286**, 18664–18672.

29. Chiang, P.M., Ling, J., Jeong, Y.H., Price, D.L., Aja, S.M. and Wong, P.C. (2010) Deletion of TDP-43 down-regulates Tbc1d1, a gene linked to obesity, and alters body fat metabolism. *Proc. Natl. Acad. Sci. USA*, **107**, 16320–16324.

30. Kraemer, B.C., Schuck, T., Wheeler, J.M., Robinson, L.C., Trojanowski, J.Q., Lee, V.M. and Schellenberg, G.D. (2010) Loss of murine TDP-43 disrupts motor function and plays an essential role in embryogenesis. *Acta. Neuropathol.*, **119**, 409–419.

31. Sephton, C.F., Good, S.K., Atkin, S., Dewey, C.M., Mayer, P. 3rd, Herz, J. and Yu, G. (2010) TDP-43 is a developmentally regulated protein essential for early embryonic development. *J. Biol. Chem.*, **285**, 6826–6834.

32. Wu, L.S., Cheng, W.C., Hou, S.C., Yan, Y.T., Jiang, S.T. and Shen, C.K. (2010) TDP-43, a neuro-pathosignature factor, is essential for early mouse embryogenesis. *Genesis*, **48**, 56–62.

33. Xu, Y.F., Gendron, T.F., Zhang, Y.J., Lin, W.L., D'Alton, S., Sheng, H., Casey, M.C., Tong, J., Knight, J., Yu, X. *et al.* (2010) Wild-type human TDP-43 expression causes TDP-43 phosphorylation, mitochondrial aggregation, motor deficits, and early mortality in transgenic mice. *J. Neurosci.*, **30**, 10851–10859.

34. Freibaum, B.D., Chitta, R.K., High, A.A. and Taylor, J.P. (2010) Global analysis of TDP-43 interacting proteins reveals strong association with RNA splicing and translation machinery. *J. Proteome Res.*, **9**, 1104–1120.

35. Kuo, P.H., Doudeva, L.G., Wang, Y.T., Shen, C.K. and Yuan, H.S. (2009) Structural insights into TDP-43 in nucleic-acid binding and domain interactions. *Nucleic Acids Res.*, **37**, 1799–1808.

36. Polymenidou, M., Lagier-Tourenne, C., Hutt, K.R., Huelga, S.C., Moran, J., Liang, T.Y., Ling, S.C., Sun, E., Wancewicz, E., Mazur, C. *et al.* (2011) Long pre-mRNA depletion and RNA missplicing contribute to neuronal vulnerability from loss of TDP-43. *Nat. Neurosci.*, **14**, 459–468.

37. Tollervey, J.R., Curk, T., Rogelj, B., Briese, M., Cereda, M., Kayikci, M., Konig, J., Hortobagyi, T., Nishimura, A.L., Zupunski, V. *et al.* (2011) Characterizing the RNA targets and position-dependent splicing regulation by TDP-43. *Nat. Neurosci.*, **14**, 452–458.

38. Ishihara, T., Ariizumi, Y., Shiga, A., Kato, T., Tan, C.F., Sato, T., Miki, Y., Yokoo, M., Fujino, T., Koyama, A. *et al.* (2013) Decreased number of Gemini of coiled bodies and U12 snRNA level in amyotrophic lateral sclerosis. *Hum. Mol. Genet.*, **22**, 4136–4147.

39. Bose, J.K., Wang, I.F., Hung, L., Tarn, W.Y. and Shen, C.K. (2008) TDP-43 overexpression enhances exon 7 inclusion during the survival of motor neuron pre-mRNA splicing. *J. Biol. Chem.*, **283**, 28852–28859.

40. Buratti, E., Dork, T., Zuccato, E., Pagani, F., Romano, M. and Baralle, F.E. (2001) Nuclear factor TDP-43 and SR proteins promote in vitro and in vivo CFTR exon 9 skipping. *EMBO J.*, **20**, 1774–1784.

41. Fiesel, F.C., Weber, S.S., Supper, J., Zell, A. and Kahle, P.J. (2012) TDP-43 regulates global translational yield by splicing of exon junction complex component SKAR. *Nucleic Acids Res.*, **40**, 2668–2682.

42. Shiga, A., Ishihara, T., Miyashita, A., Kuwabara, M., Kato, T., Watanabe, N., Yamahira, A., Kondo, C., Yokoseki, A., Takahashi, M. *et al.* (2012) Alteration of POLDIP3 splicing associated with loss of function of TDP-43 in tissues affected with ALS. *PLoS One*, **7**, e43120.

43. Colombrita, C., Onesto, E., Megiorni, F., Pizzuti, A., Baralle, F.E., Buratti, E., Silani, V. and Ratti, A. (2012) TDP-43 and FUS RNA-binding proteins bind distinct sets of cytoplasmic messenger RNAs and differently regulate their post-transcriptional fate in motoneuron-like cells. *J. Biol. Chem.*, **287**, 15635–15647.

44. Rabin, S.J., Kim, J.M., Baughn, M., Libby, R.T., Kim, Y.J., Fan, Y., Libby, R.T., La Spada, A., Stone, B. and Ravits, J. (2010) Sporadic ALS has compartment-specific aberrant exon splicing and altered cell-matrix adhesion biology. *Hum. Mol. Genet.*, **19**, 313–328.

45. Burghes, A.H. and Beattie, C.E. (2009) Spinal muscular atrophy: why do low levels of survival motor neuron protein make motor neurons sick? *Nat. Rev. Neurosci.*, **10**, 597–609.

46. Jady, B.E., Darzacq, X., Tucker, K.E., Matera, A.G., Bertrand, E. and Kiss, T. (2003) Modification of Sm small nuclear RNAs occurs in the nucleoplasmic Cajal body following import from the cytoplasm. *EMBO J.*, **22**, 1878–1888.

47. Mao, Y.S., Zhang, B. and Spector, D.L. (2011) Biogenesis and function of nuclear bodies. *Trends Genet.*, **27**, 295–306.

48. Tsuiji, H., Iguchi, Y., Furuya, A., Kataoka, A., Hatsuta, H., Atsuta, N., Tanaka, F., Hashizume, Y., Akatsu, H., Murayama, S. *et al.* (2013)

Spliceosome integrity is defective in the motor neuron diseases ALS and SMA. *EMBO Mol. Med.*, **5**, 221–234.

49. van Blitterswijk, M. and Landers, J.E. (2010) RNA processing pathways in amyotrophic lateral sclerosis. *Neurogenetics*, **11**, 275–290.

50. Inukai, Y., Nonaka, T., Arai, T., Yoshida, M., Hashizume, Y., Beach, T.G., Buratti, E., Baralle, F.E., Akiyama, H., Hisanaga, S. *et al.* (2008) Abnormal phosphorylation of Ser409/410 of TDP-43 in FTLD-U and ALS. *FEBS Lett.*, **582**, 2899–2904.

51. Hirai, S., Miwa, A., Ohtaka-Maruyama, C., Kasai, M., Okabe, S., Hata, Y. and Okado, H. (2012) RP58 controls neuron and astrocyte differentiation by downregulating the expression of Id1–4 genes in the developing cortex. *EMBO J.*, **31**, 1190–1202.

52. Fujiki, T., Miura, T., Maura, M., Shiraishi, H., Nishimura, S., Imada, Y., Uehara, N., Tashiro, K., Shirahata, S. and Katakura, Y. (2007) TAK1 represses transcription of the human telomerase reverse transcriptase gene. *Oncogene*, **26**, 5258–5266.

Original Investigation

Lower Motor Neuron Involvement in TAR DNA-Binding Protein of 43 kDa–Related Frontotemporal Lobar Degeneration and Amyotrophic Lateral Sclerosis

Yuichi Riku, MD; Hirohisa Watanabe, MD; Mari Yoshida, MD; Shinsui Tatsumi, MD; Maya Mimuro, MD; Yasushi Iwasaki, MD; Masahisa Katsuno, MD; Yohei Iguchi, MD; Michihito Masuda, MD; Jo Senda, MD; Shinsuke Ishigaki, MD; Tsuyoshi Udagawa, PhD; Gen Sobue, MD

IMPORTANCE TAR DNA-binding protein of 43 kDa (TDP-43) plays a major role in the pathogenesis of frontotemporal lobar degeneration (FTLD) and amyotrophic lateral sclerosis (ALS). Although a pathological continuity between FTLD and ALS has been suggested, the neuropathological changes of the lower motor neuron (LMN) systems have not been assessed in TDP-43–associated FTLD (FTLD-TDP), to our knowledge.

OBJECTIVE To investigate a pathological continuity between FTLD-TDP and ALS by comparing their respective neuropathological changes in the motor neuron system.

DESIGN AND SETTING A retrospective clinical medical record review and a semiquantitative neuropathological evaluation of the cranial motor nerve nuclei and spinal cord were conducted at autopsy. We included 43 patients with sporadic FTLD-TDP, type A, B, or C, from 269 consecutively autopsied patients with TDP-43 proteinopathy. Patients were categorized as having FTLD without ALS, FTLD-ALS (onset of FTLD symptoms/signs preceded those of ALS), or ALS-FTLD (onset of ALS symptoms/signs preceded those of FTLD).

MAIN OUTCOMES AND MEASURES Neuronal TDP-43 pathological changes and neuronal loss.

RESULTS Forty-three patients were included in the clinical analysis, and 29 from whom spinal cords were obtained were included in the neuropathological analysis. Survival time was significantly shorter in the FTLD-ALS and ALS-FTLD groups than in the FTLD without ALS group ($P < .001$). At neuropathological examination, 89% of patients in the FTLD without ALS group showed aggregations of TDP-43 in the spinal motor neurons. The LMN loss was most severe in ALS-FTLD, followed by FTLD-ALS and FTLD without ALS. All the patients with type A or C FTLD-TDP were included in the FTLD without ALS group, and all those with type B pathological changes were in the FTLD-ALS or the ALS-FTLD group. Lower motor neuron loss and TDP-43–positive skeinlike inclusions were observed in all pathological subtypes.

CONCLUSIONS AND RELEVANCE The LMN systems of FTLD-TDP frequently exhibit neuropathological changes corresponding to ALS. Thus, a pathological continuity between FTLD-TDP and ALS is supported at the level of the LMN system.

– 148 –

rontotemporal lobar degeneration (FTLD) is a sporadic or familial neurodegenerative disease that clinically encompasses frontotemporal dementia, language disorder, and motor symptoms.[1] Immunohistochemical profiles show that approximately half of patients with FTLD present with tau-positive disease, but the other half primarily exhibit an accumulation of TAR DNA-binding protein of 43 kDa (TDP-43), referred to as FTLD-TDP.[2-5] Currently, the cortical TDP-43 pathological changes in sporadic FTLD-TDP are classified into 3 subtypes: A, B, and C.[6-8]

TAR DNA-binding protein of 43 kDa is also a major disease protein in amyotrophic lateral sclerosis (ALS), which is characterized by upper motor neuron and lower motor neuron (LMN) involvement.[9] The pathological features of LMN involvement in ALS include neuronal loss, gliosis, TDP-43-positive neuronal inclusions with skeinlike or round shapes and glial inclusions, and Bunina bodies.[10]

Some patients exhibit symptoms of both ALS and FTLD, and the cerebral cortices of patients with FTLD and ALS almost always show type B TDP-43 changes.[7,11-13] Thus, a pathological continuity between FTLD and ALS has been proposed based on brain TDP-43 pathological findings. Studies of the cerebral cortex, including the motor cortex, and subcortical gray matter have shown common TDP-43 pathological findings in FTLD, FTLD with ALS, and ALS.[12,14-17] However, the neuropathological features of LMN systems in FTLD-TDP have not been investigated comprehensively, particularly in the spinal cord, although characterization of these features is necessary to confirm the pathological relationship between FTLD and ALS.

In this study, we investigated LMN pathological findings in patients with sporadic FTLD-TDP who clinically demonstrated FTLD, FTLD with ALS, or ALS. We also investigated the correlation between TDP-43 pathological subtypes (type A, B, and C) and LMN involvement to further elucidate the continuity of FTLD and ALS.

Methods

Study Patients
We enrolled 269 consecutively autopsied patients with sporadic and adult-onset FTLD, FTLD with ALS, or ALS in which pathological aggregation of TDP-43 was confirmed at the Department of Neuropathology, Institute for Medical Science of Aging, Aichi Medical University, from 1988 to 2012. All patients had been clinically evaluated by neurological experts in the affiliated hospitals of Nagoya University School of Medicine or Aichi Medical University. Permission to perform an autopsy and archive the nervous system tissues for research purposes was obtained from family members after death. The clinical data on the included patients were obtained from case notes made at diagnosis and at an advanced stage of illness. We initially excluded 216 of the 269 patients because they did not present clinical FTLD symptoms. In 53 patients, FTLD or FTLD with ALS was diagnosed according to the diagnostic criteria of FTLD and ALS.[1,18] Moreover, we subclassified FTLD with ALS into FTLD-ALS

(onset of FTLD symptoms/signs preceded those of ALS) and ALS-FTLD (onset of ALS symptoms/signs preceded those of FTLD) groups.

The enrolled patients were categorized into 3 groups: FTLD without ALS, FTLD-ALS, and ALS-FTLD. The FTLD symptoms were categorized into 2 groups: behavior-variant frontotemporal dementia and language impairments.[14] The LMN symptoms/signs were defined by progressive muscular weakness, muscular atrophy, fasciculation, or electromyographic findings. We excluded patients with Alzheimer disease-associated neurofibrillary pathological abnormalities that were more advanced than Braak stage IV,[19] those with argyrophilic grain disease, and those with invalid clinical data. Finally, 43 patients were included in the clinical analysis (11 with FTLD without ALS, 9 with FTLD-ALS, and 23 with ALS-FTLD). For comparison, we prepared 13 age-matched controls (mean [SD] age at death, 68.2 [6.9] years) who had no diagnosis of any neurodegenerative disease, dementia, or cerebrovascular disease.

Clinical Analyses
The information regarding sex, age at onset, disease duration, and duration between onset of FTLD and ALS was collected from clinical notes. Causes of death were classified as respiratory failure due to respiratory muscle weakness, pneumonia, or other. The last category comprised systemic diseases other than respiratory failure or pneumonia, including cancer, ileus, infections, and renal failure. Information on the subtypes of dementia, clinical data on motor symptoms, and electromyographic results were also collected.

Pathological Evaluations
For the neuropathological analysis, we excluded patients who had received a respirator/tracheotomy (n = 11) or whose spinal cord was not available (n = 3). In total, 29 patients were included in the neuropathological analysis and divided into 3 groups: FTLD without ALS (n = 9), FTLD-ALS (n = 8), and ALS-FTLD (n = 12). The tissues were fixed in 20% neutral-buffered formalin. The paraffin-embedded tissue blocks were cut at a thickness of 4.5 μm. We evaluated sections from the spinal cord and whole brain. The whole spinal cord was examined at each segmental level, but only the cervical cord was available in 3 patients and the sacral cord was not available in another 3.

For routine neuropathological examinations, the sections were stained with hematoxylin-eosin and Klüver-Barrera. Immunohistochemical studies were performed using a standard polymer-based method with the EnVision Kit or anti-goat immunoglobulin (Dako). As primary antibodies, we used antibodies to the following: anti-ubiquitin (ubiquitin, monoclonal mouse, 1:250; Millipore), anti-TDP-43 (TARDBP, polyclonal rabbit, 1:2500; ProteinTech), anti-phosphorylated TDP-43 (pTDP-43 ser409/410, polyclonal rabbit, 1:2500; CosmoBio), anti-phosphorylated tau (AT-8, monoclonal mouse, 1:4000; Innogenetics), anti-β-amyloid (β-amyloid 6F/3D, monoclonal mouse, 1:100; Dako), anti-CD68 (CD68, monoclonal mouse, 1:200; Dako), anti-cystatin C (cystatin C, polyclonal rabbit, 1:200; Dako), p62 N-terminal (p62N, polyclonal

- 149 -

guinea pig, 1:100; Progen), anti-ubiquilin 2 (UBQLN-2 5F5, monoclonal mouse, 1:5000; Abnova), and anti-choline acetyltransferase (ChAT, polyclonal goat, 1:100; Millipore). Diaminobenzidine (Wako) was used as the chromogen.

Antigens were retrieved with trypsin for anti-CD68 immunohistochemistry and with 95°C 3 mmol/L citrate buffer at 95°C for 20 minutes, followed by 5-minute incubation in 98% formic acid for anti-p62N, anti-TDP-43, anti-pTDP-43, and anti-ChAT immunohistochemistry. To confirm the presence of TDP-43-positive inclusions within the cholinergic motor neurons, we performed double immunohistochemistry using anti-pTDP-43 and anti-ChAT antibodies. Spinal cord specimens were prepared from 3 patients with type A, 3 with type B, and 2 with type C. Initially, the specimens were immunostained with the anti-ChAT and anti-goat immunoglobulin antibodies and diaminobenzidine. The anti-ChAT antibody was inactivated in distilled water at 100°C for 20 minutes, followed by immunohistochemistry with pTDP-43 and violet pigmentation using a VIP Peroxidase Substrate Kit (SK-4600; Vector).

For the semiquantitative neuropathological analysis, 2 investigators (Y.R. and M.Y.) observed the specimens containing the facial and hypoglossal nuclei and the anterior horn of the spinal cord. They evaluated the severity of LMN neuropathological changes that are indicative of ALS (neuronal loss, gliosis, aggregation of macrophages, TDP-43-immunopositive neuronal inclusions, and Bunina bodies) and graded neuronal loss and gliosis using Klüver-Barrera and hematoxylin-eosin staining. The investigators also evaluated the aggregations of macrophages rather than rod-shaped microglia using anti-CD68 immunohistochemistry and identified Bunina bodies using hematoxylin-eosin staining and anti-cystatin C immunohistochemistry. They scored the severity of neuronal loss and gliosis as grade 0 (none), 1 (mild), 2 (moderate), or 3 (severe) (eFigure 1 in Supplement. The appearance of TDP-43-positive inclusions was scored as grade 0 (none), grade 1 (1-5 neuronal inclusions per 5 fields; ×20 objective), grade 2 (6-10 inclusions), or grade 3 (≥11 inclusions) using anti-pTDP-43 immunohistochemistry.

Pathological cortical TDP-43 subtypes were identified according to current neuropathological criteria, using specimens from the frontal lobes, temporal lobes, and hippocampus.[5] For FTLD-TDP, type A was defined as the presence of neuronal cytoplasmic inclusions predominantly in the neocortex layer 2 and short dystrophic neurites; type B, as a predominance of neuronal cytoplasmic inclusions in all cortical layers; and type C, as a predominance of long dystrophic neurites in layer 2 and cytoplasmic inclusions in the dentate granular cells of the hippocampus. Our patient series did not include type D, which is characterized by numerous short dystrophic neurites and neuronal intranuclear inclusions in association with valosin-containing protein gene mutations. We also evaluated pathological changes in the upper motor neuron systems that include the primary motor cortex and corticospinal tract (CST). We evaluated the presence or absence of neuronal loss and gliosis in the primary motor cortex and myelin pallor, as well as the aggregation of macrophages in the CST.

Immunohistochemical Screening of Hexanucleotide Repeat Expansion Sequence in Chromosome 9 Open Reading Frame 72

Our study focused on sporadic FTLD-TDP, and patients with familial histories of FTLD or ALS, dementia, or other neurodegenerative diseases were excluded. However, FTLD or ALS associated with chromosome 9 open reading frame 72 (C9ORF72) hexanucleotide expansion exhibits pathological aggregation of TDP-43 and, in some cases, low penetration,[20,21] although these mutations are extremely rare in Japan.[22] It was recently reported that the pattern of ubiquilin abnormalities in ALS and FTLD corresponds well with the presence of C9ORF72 hexanucleotide expansion.[23] The UBQLN-2-positive, p62-positive, but TDP-43-negative thick dystrophic neurites are abundantly present in patients with C9ORF72 hexanucleotide expansion, predominantly in the hippocampus and cerebellum. Because the materials for a genetic study were not available for a large proportion of our patients, we histologically screened C9ORF72 hexanucleotide expansion with the absence of UBQLN-2 and p62N-positive thick dystrophic neurites in the temporal lobes and cerebella of all patients.

Statistical Analysis

The Mann-Whitney test was applied to continuous variables between 2 groups, and the Kruskal-Wallis test was applied to the analysis of continuous variables among 3 groups. The χ^2 test was used for categorized variables among 3 groups. Spearman rank correlation coefficient analyses were applied to univariate correlations between the clinical groups and severity of pathological changes. Survival curves were constructed using the Kaplan-Meier method. The end point of clinical course was defined as death or the introduction of a respirator or tracheotomy. The significance level for all comparisons was set at $P < .05$. All statistical tests were 2 sided and were conducted using the PASW 18.0 program (IBM SPSS).

Results

Clinical Analysis

Patient characteristics are summarized in the **Table**. The mean (SD) time from symptom onset to death or respirator or tracheotomy administration was 50.5 (58.4) months across all patients. The survival time from symptom onset did not differ significantly between the FTLD-ALS and ALS-FTLD groups but was significantly shorter for the FTLD without ALS group than for the FTLD-ALS or ALS-FTLD group (**Figure 1** and Table; $P < .001$). The most common cause of death for the ALS-FTLD and FTLD-ALS groups was respiratory failure, but patients with FTLD without ALS commonly died of other systemic diseases ($P < .001$). Frequencies of dementia subtypes did not significantly differ between the clinical groups.

With regard to motor symptoms/signs, 3 patients in the FTLD without ALS group had hyperreflexia, 1 had the Babinski sign, and 1 had spasticity, but none had a clinical diagnosis of progressive lateral sclerosis (PLS) according to the published diagnostic criteria of PLS.[24] Patients with FTLD-ALS or

- 150 -

Table. Clinical and Demographic Patient Characteristics

Characteristic	Patient Group			P Value
	FTLD Without ALS (n = 11)	FTLD-ALS (n = 9)	ALS-FTLD (n = 23)	
Sex, No. female/male[a]	8/3	3/6	10/13	.16
Age at onset, mean (SD), y[b]	62.4 (9.4)	58.2 (11.3)	61.2 (9.5)	.79
Clinical duration without respirator or tracheotomy, median (range), mo[c]	84.0 (47.0-360.0)	28.0 (7.0-60.0)	22.0 (7.0-71.0)	<.001
Duration between FTLD and ALS, median (range), mo[d]		18.0 (4.0-48.0)	19.0 (0-60.0)	.92
Patients with tracheotomy, No. (%)[a]	0	0	2 (9)	.40
Patients with respirators, No. (%)[a]	0	1 (11)	8 (35)	.047
Duration with respirator or tracheotomy, median (range), mo		30.0	39.0 (1.0-141.0)	...
Causes of death, No. (%)[a]				
Respiratory failure	0	6 (67)	20 (87)	<.001
Pneumonia	3 (27)	3 (33)	3 (13)	.37
Other	8 (73)	0	0	<.001
Subtypes of dementia, No. (%)				
Behavior-variant FTD	7 (64)	7 (78)	19 (83)	.29
Language impairments	4 (36)	2 (22)	4 (17)	.62
Motor symptoms/signs, No. (%)				
Muscle weakness[a]	0	9 (100)	23 (100)	<.001
Muscle atrophy	0	7 (78)	22 (96)	<.001
Fasciculation	0	4 (44)	15 (65)	.002
Hyperreflexia	3 (27)	5 (56)	17 (74)	.009
Babinski sign	1 (9)	4 (44)	3 (13)	.08
Spasticity	1 (9)	0	1 (4)	.63
Electromyography, No. (%)				
Total examined	2 (18)	4 (82)	21 (91)	...
Active denervation[a]	0	3 (75)	12 (57)	.054

Abbreviations: ALS, amyotrophic lateral sclerosis; ALS-FTLD, onset of ALS symptoms/signs preceding those of frontotemporal lobar degeneration (FTLD); ellipses, not significant; FTD, frontotemporal dementia; FTLD-ALS, onset of FTLD symptoms/signs preceding those of ALS.

[a] χ^2 Test.

[b] Kruskal-Wallis test.

[c] Log-rank test.

[d] Mann-Whitney test.

ALS-FTLD generally exhibited both upper motor neuron and LMN symptoms/signs except for 3 who exhibited only LMN symptoms/signs. Based on the electromyographic data, active denervation potentials (positive sharp waves and fibrillation potentials[18]) were identified in 3 patients with FTLD-ALS and 12 with ALS-FTLD but not in any of those with FTLD without ALS.

Pathological Evaluations of the LMN System

The results of semiquantitative pathological evaluations of the 3 clinical groups are summarized in **Figure 2**. In the FTLD without ALS group, 8 of 9 patients (89%) showed pTDP-43-positive neuronal inclusions. In addition, neuronal loss and gliosis in the spinal anterior horns were observed in 5 of 11 patients (45%) and Bunina bodies were present in 4 (36%). The pathological changes in LMN systems were most severe in the ALS-FTLD group, followed by the FTLD-ALS group, and were rather mild in the FTLD without ALS group. Among control patients, 1 had a pTDP-43-positive glial inclusion in the lumbar anterior horn, but this patient did not show neuronal loss, gliosis, or Bunina bodies (eFigure 2 in Supplement).

Figure 1. Survival by Clinical Group
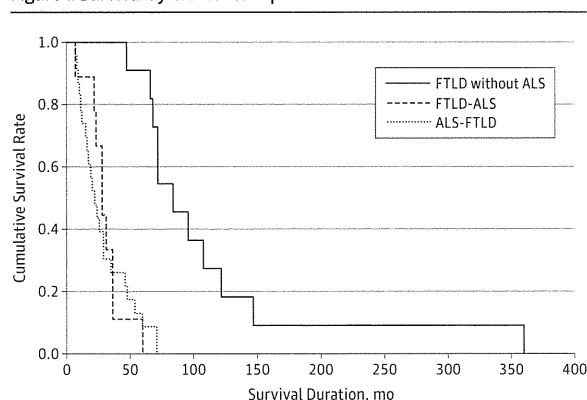
Kaplan-Meier plot showing the survival rates of patients with frontotemporal lobar degeneration (FTLD) without amyotrophic lateral sclerosis (ALS) (solid line; n = 11), those in whom the onset of FTLD symptoms/signs preceded those of ALS (FTLD-ALS) (dashed line; n = 9), and those in whom the onset of ALS symptoms/signs preceded those of FTLD (ALS-FTLD) (dotted line; n = 23). Survival times were significantly shorter in patients with FTLD without ALS than in those with FTLD-ALS or ALS-FTLD ($P < .001$).

- 151 -

Figure 2. Semiquantitative Evaluations of Pathological Changes by Clinical Group

Patients	FTLD Without ALS									FTLD-ALS								ALS-FTLD												P Values	r Values
	1	2	3	4	5	6	7	8	9	10	11	12	13	14	15	16	17	18	19	20	21	22	23	24	25	26	27	28	29		
Clinical duration, mo	47	66	84	108	147	360	68	96	122	22	23	28	28	31	36	36	60	7	8	9	10	16	20	22	24	26	54	60	71		
Neuronal loss																															
Facial nuclei																														<.01	0.730
Hypoglossal nuclei																														<.01	0.823
Anterior horn of Cx																														<.01	0.804
Anterior horn of Tx																														<.01	0.768
Anterior horn of Lx																														<.01	0.856
Anterior horn of Sx																														<.01	0.880
Gliosis																															
Facial nuclei																														<.01	0.768
Hypoglossal nuclei																														<.01	0.828
Anterior horn of Cx																														<.01	0.730
Anterior horn of Tx																														<.01	0.740
Anterior horn of Lx																														<.01	0.878
Anterior horn of Sx																														<.01	0.904
pTDP-43-positive neuronal inclusions																															
Facial nuclei																														<.01	0.729
Hypoglossal nuclei																														.08	0.348
Anterior horn of Cx																														<.01	0.511
Anterior horn of Tx																														<.05	0.403
Anterior horn of Lx																														<.05	0.412
Anterior horn of Sx																														<.05	0.458
Aggregation of macrophages																															
Facial nuclei																														<.01	0.518
Hypoglossal nuclei																														<.01	0.634
Anterior horn of Cx																														0.78	0.073
Anterior horn of Tx																														<.05	0.435
Anterior horn of Lx																														<.01	0.721
Anterior horn of Sx																														<.01	0.751
Bunina bodies																															
Brain TDP-43 disease type	A	A	A	A	A	A	C	C	C	B	B	B	B	B	B	B	B	B	B	B	B	B	B	B	B	B	B	B	B		

Findings shown include the severity of neuronal loss, gliosis, phosphorylated TAR DNA-binding protein of 43 kDa (pTDP-43) pathological changes, and aggregations of macrophages and the presence of Bunina bodies in the lower motor neuron systems. The severity of each pathological change was graded as 0 (none [–, not colored]), 1 (mild [+, green]), 2 (moderate [++, yellow]), or 3 (severe [+++, red]). Neuropathological changes became increasingly severe in those in whom amyotrophic lateral sclerosis (ALS) symptoms/signs preceded those of frontotemporal lobar degeneration (FTLD; ALS-FTLD), as well as the FTLD-ALS (FTLD symptoms/signs preceding those of ALS) and FTLD without ALS groups (Spearman rank order). Cx indicates cervical cord; Lx, lumbar cord; NA, not assessed; Sx, sacral cord; TDP-43, TAR DNA-binding protein of 43 kDa; and Tx, thoracic cord.

According to cortical TDP-43 pathological findings,[5] 29 patients were classified into 3 subtypes: A (n = 6), B (n = 20), or C (n = 3). Patients with FTLD without ALS showed type A or C disease, whereas those with FTLD-ALS or ALS-FTLD all showed type B disease (Figure 2 and **Figure 3**). For all the subtypes, the LMN system showed neuropathological changes that were indicative of ALS, including pTDP-43-positive neuronal and glial inclusions, neuronal loss, and gliosis. In patients with type A disease (**Figure 4A-H**), the severity of neuronal loss and gliosis in LMN systems ranged from none to moderate. Five patients (83%) in this group had pTDP-43-positive, skeinlike cytoplasmic and/or nuclear inclusions (Figure 4B and C), and 4 (67%) had Bunina bodies (Figure 4E and F) in the LMNs.

All 20 patients in the type B group (Figure 4I-L) showed neuronal loss, gliosis, and pTDP-43-positive skeinlike cytoplasmic inclusions in the LMN systems, and 18 (90%) had Bunina bodies. Among the 3 patients with type C disease (Figure 4M-P), 1 (33%) had mild loss of the LMNs (Figure 4M), and all 3 (100%) had pTDP-43-positive skeinlike cytoplasmic inclusions in the LMNs (Figure 4N). Unlike patients with the

other subtypes, those with type C disease lacked Bunina bodies. Moreover, thick dystrophic neurites were prominent in the spinal anterior horn in patients with type A or C disease but rarely present in those with type B disease (Figure 4G and O). These dystrophic neurites were larger in diameter (8-12 μm) than those found in the cortices. In a double immunohistochemical analysis, pTDP-43-positive inclusions were found within the cytoplasm of ChAT-positive neurons in patients with type A, B, and C disease (Figure 4H, L, and P).

Pathological Evaluations of the Upper Motor Neuron System

In the primary motor cortex, neuronal loss and gliosis were evident in 5 patients with FTLD without ALS (56%), 2 with FTLD-ALS (25%), and 3 with ALS-FTLD (25%). Myelin pallor in the CST was evident in 6 patients with FTLD without ALS (67%), 1 with FTLD-ALS (12%), and 2 with ALS-FTLD (17%). Aggregations of macrophages in the CST were evident in 4 patients with FTLD without ALS (44%), 5 with FTLD-ALS (62%), and 6 with ALS-FTLD (50%).

– 152 –

Figure 3. Semimacroscopic Appearances and Brain Pathological Findings in Patients With Type A, B, and C Pathological Changes
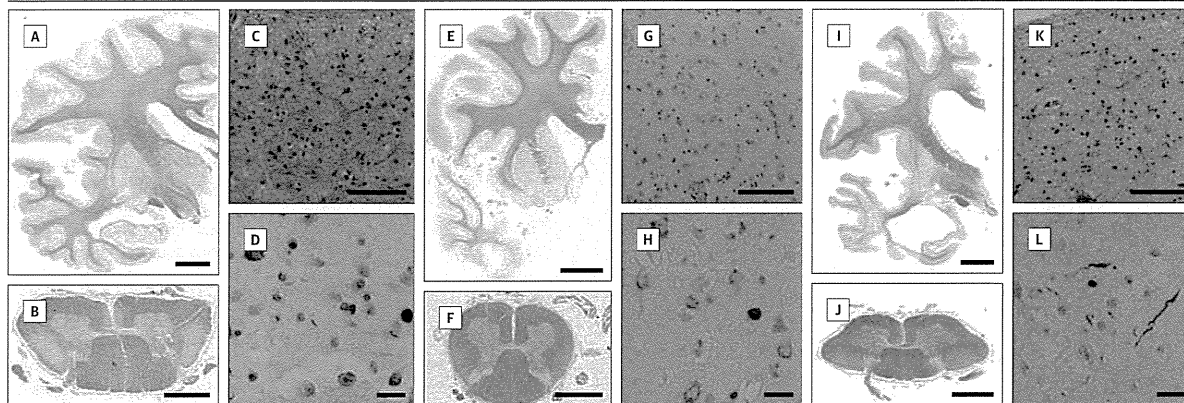
Findings in patients with type A (A-D), B (E-H), and C (I-L) pathological changes. In a patient with type A pathological change, cerebral coronal sections showed cortical atrophy of the parasylvian region (A). Transverse section of the cervical cord showed marked myelin pallor in the corticospinal tract (B). Microscopically, the frontal cortices showed marked neuronal loss (C) and phosphorylated TAR DNA-binding protein of 43 kDa (pTDP-43)-positive neuronal inclusions and short dystrophic neurites (D). In a patient with type B pathological change, the cerebral cortex showed severe temporal atrophy (E), neuronal loss (G), and pTDP-43-positive neuronal inclusions (H). The corticospinal tract showed mild myelin pallor (F). In a patient with type C patholgoical change, the frontal and temporal cortices showed severe atrophy (I), marked neuronal loss (K), and pTDP-43-positive long dystrophic neurites (L). The corticospinal tract showed marked myelin pallor (J). Klüver-Barrera staining (A, B, E, F, I, and J), hematoxylin-eosin staining (C, G, and K), and pTDP-43 immunohistochemistry (D, H, and L) were performed. Scale bars represent 1 cm (A, E, and I), 3 mm (B, F, and J), 100 μm (C, G, and K), and 20 μm (D, H, and L). Original magnifications are ×1 (A, B, E, F, I, and J), ×200 (C, G, and K), and ×400 (D, H, and L).

Anti-UBQLN-2 and Anti-p62N Immunohistochemistry

No patients showed any cerebellar UBQLN-2-positive or p62N-positive structures. In the temporal lobes, UBQLN-2-positive structures were occasionally observed in 8 patients, but abundant, thick, and aggregatelike structures, which are found in patients with C9ORF72 expansions, were not observed (eFigure 3 in Supplement). We presumed that our patients did not have C9ORF72 expansions.

Discussion

Our study demonstrated that pTDP-43-associated pathological changes were common in the spinal anterior horns of the FTLD without ALS, FTLD-ALS, and ALS-FTLD groups. Neuronal loss and gliosis were most severe among the ALS-FTLD group, followed by the FTLD-ALS and then the FTLD without ALS groups. Our results clearly demonstrated the pathological continuum among TDP-43-associated FTLD and ALS, even at the LMN level.

Although the FTLD without ALS group that lacked LMN symptoms showed a loss of LMNs, the degree of neuronal loss and TDP-43 disease were generally mild in this group. Experiment data using ALS mouse models revealed that symptoms developed when approximately 29% of spinal motor neurons were lost.[25] Further investigation will be needed to clarify whether LMN involvement occurs in a later stage of illness or progresses very slowly compared with cerebral involvement in FTLD without ALS.

Our results revealed that the FTLD-TDP types A, B, and C were associated with neuropathological changes corresponding to ALS in the spinal motor neurons. The severity of neuronal loss and pTDP-43 disease in the spinal motor neurons

may differ quantitatively among these neuropathological subtypes. Based on cortical TDP-43 pathological findings, patients in the type B group had severe neuronal loss and diffuse pTDP-43-positive neuronal inclusions, which were entirely identical to ALS, whereas these changes were mild in the type C group. In type A, LMN pathological findings were diverse regardless of clinical duration; their severity and extension may be heterogeneous among patients with type A disease, unlike those with type B or C disease. Indeed, type A disease has also been identified in the FTLD with ALS phenotype in sporadic or familial (C9ORF72 expansion or progranulin gene mutations) form.[2,5,21,26] Dystrophic neurites were prominent in the spinal anterior horn of patients with type A or C disease. In our patient series, Bunina bodies were observed in most patients with type A or B disease but were absent in those with type C disease, findings consistent with those of previous studies.[3,17]

Several studies have demonstrated that some patients with FTLD-TDP, particularly type C, showed marked CST degeneration.[3,11,17,27] We also observed a marked myelin pallor in the CST in 67% of patients with FTLD without ALS, 12% with FTLD-ALS, and 16% with ALS-FTLD (50% for type A, 15% for type B, and 100% for type C). Some patients showed neuronal loss or gliosis in the primary motor cortex to varying extents. Furthermore, patients with FTLD without ALS often exhibited severe degenerative changes in broad areas of the frontal cortices. The broad involvement of the frontal lobes might also contribute to the CST degeneration because CST fibers arise not only from the primary motor cortex but also from the premotor cortex and supplementary motor areas.[28]

Two limitations of our study is that the evaluation of slight or very mild muscle weakness was not completed and that there were few patients with electromyographic data in

- 153 -

Figure 4. Pathological Findings of Spinal Motor Neuron in Subtypes of TAR DNA-Binding Protein of 43 kDa (TDP-43) Pathological Changes
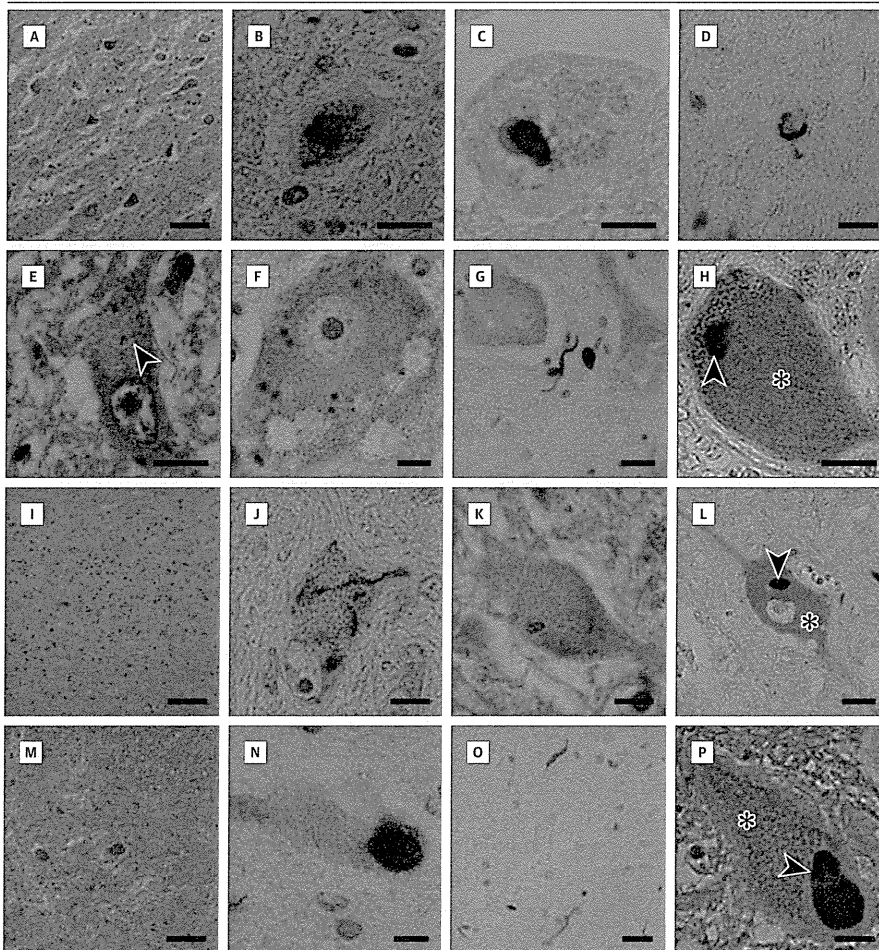
Patients with type A (A-H), type B (I-L), and type C (M-P) pathological changes. A patient with type A pathological change showed mild neuronal loss (A), phosphorylated TDP-43 (pTDP-43)–positive skeinlike cytoplasmic inclusions (B), nuclear inclusions (C), and glial inclusions (D), Bunina bodies (E [arrow] and F) in the spinal anterior horn, and dystrophic neurites (G). In a patient with type B pathological change, neuronal loss (I), pTDP-43–positive skeinlike cytoplasmic inclusions (J), and Bunina bodies (K) were markedly observed. In a patient with type C pathological change, the spinal anterior horn showed mild neuronal loss (M), pTDP-43–positive skeinlike cytoplasmic inclusions (N), and dystrophic neurites (O). Double immunohistochemistry for choline acetyltransferase (ChAT) and pTDP-43 revealed cytoplasmic inclusions (violet [arrows]) present within the cytoplasm of a ChAT-positive spinal motor neuron (brown [asterisks]) of patients with type A (H), B (L), or C (P) pathological change. Hematoxylin-eosin staining (A, E, I, K, and M), pTDP-43 immunohistochemistry (B, C, D, G, J, N, and O), cystatin-C (F), and double immunohistochemical analysis for pTDP-43 and ChAT (H, L, and P) were performed. Scale bars represent 100 (A, I, and M), 20 (G, L, and O), and 10 (B-F, H, J, K, N, and P) μm. Original magnifications are ×100 (A, I, and M), ×400 (G, L, and O), and ×1000 (B-F, H, J, K, N, and P).

the FTLD without ALS group. However, our clinical data demonstrated that patients with FTLD without ALS had significantly longer survival times than those with FTLD-ALS or ALS-FTLD. These prognostic data correspond well to previous results.[29,30] In addition, the causes of death differed considerably between the FTLD without ALS group and the FTLD-ALS and ALS-FTLD groups. Respiratory failure was observed in patients with FTLD-ALS or ALS-FTLD but not in those with FTLD without ALS, and respiratory failure was strongly associated with severity of LMN loss. These results support the view that classification of FTLD based on the presence of LMN involvement was applicable in this study.

In conclusion, the LMN systems of FTLD-TDP generally show neuropathological changes that are indicative of ALS, although the severity of pathological changes differs among clinical phenotypes or subtypes of cortical TDP-43 disease. A pathological continuity between FTLD-TDP and ALS is supported by evidence of LMN involvement.

– 154 –

REFERENCES

1. Cairns NJ, Neumann M, Bigio EH, et al. TDP-43 in familial and sporadic frontotemporal lobar degeneration with ubiquitin inclusions. *Am J Pathol*. 2007;171(1):227-240.

2. Josephs KA, Whitwell JL, Murray ME, et al. Corticospinal tract degeneration associated with TDP-43 type C pathology and semantic dementia. *Brain*. 2013;136(pt 2):455-470.

3. Mackenzie IR, Neumann M, Bigio EH, et al. Nomenclature and nosology for neuropathologic subtypes of frontotemporal lobar degeneration: an update. *Acta Neuropathol*. 2010;119(1):1-4.

4. Whitwell JL, Jack CR Jr, Parisi JE, et al. Does TDP-43 type confer a distinct pattern of atrophy in frontotemporal lobar degeneration? *Neurology*. 2010;75(24):2212-2220.

5. Mackenzie IR, Neumann M, Baborie A, et al. A harmonized classification system for FTLD-TDP pathology. *Acta Neuropathol*. 2011;122(1):111-113.

6. Mackenzie IR, Baborie A, Pickering-Brown S, et al. Heterogeneity of ubiquitin pathology in frontotemporal lobar degeneration: classification and relation to clinical phenotype. *Acta Neuropathol*. 2006;112(5):539-549.

7. Sampathu DM, Neumann M, Kwong LK, et al. Pathological heterogeneity of frontotemporal lobar degeneration with ubiquitin-positive inclusions delineated by ubiquitin immunohistochemistry and novel monoclonal antibodies. *Am J Pathol*. 2006;169(4):1343-1352.

8. Neumann M, Sampathu DM, Kwong LK, et al. Ubiquitinated TDP-43 in frontotemporal lobar degeneration and amyotrophic lateral sclerosis. *Science*. 2006;314(5796):130-133.

9. Josephs KA, Dickson DW. Frontotemporal lobar degeneration with upper motor neuron disease/ primary lateral sclerosis. *Neurology*. 2007;69(18):1800-1801.

10. Geser F, Lee VM, Trojanowski JQ. Amyotrophic lateral sclerosis and frontotemporal lobar degeneration: a spectrum of TDP-43 proteinopathies. *Neuropathology*. 2010;30(2):103-112.

11. Snowden J, Neary D, Mann D. Frontotemporal lobar degeneration: clinical and pathological relationships. *Acta Neuropathol*. 2007;114(1):31-38.

12. Geser F, Martinez-Lage M, Robinson J, et al. Clinical and pathological continuum of multisystem TDP-43 proteinopathies. *Arch Neurol*. 2009;66(2):180-189.

13. Nishihira Y, Tan CF, Hoshi Y, et al. Sporadic amyotrophic lateral sclerosis of long duration is associated with relatively mild TDP-43 pathology. *Acta Neuropathol*. 2009;117(1):45-53.

14. Geser F, Stein B, Partain M, et al. Motor neuron disease clinically limited to the lower motor neuron is a diffuse TDP-43 proteinopathy. *Acta Neuropathol*. 2011;121(4):509-517.

15. Yoshida M. Amyotrophic lateral sclerosis with dementia: the clinicopathological spectrum. *Neuropathology*. 2004;24(1):87-102.

16. Kobayashi Z, Tsuchiya K, Arai T, et al. Clinicopathological characteristics of FTLD-TDP showing corticospinal tract degeneration but lacking lower motor neuron loss. *J Neurol Sci*. 2010;298(1-2):70-77.

17. Brooks BR, Miller RG, Swash M, Munsat TL; World Federation of Neurology Research Group on Motor Neuron Diseases. El Escorial revisited: revised criteria for the diagnosis of amyotrophic lateral sclerosis. *Amyotroph Lateral Scler Other Motor Neuron Disord*. 2000;1(5):293-299.

18. Neary D, Snowden JS, Gustafson L, et al. Frontotemporal lobar degeneration: a consensus on clinical diagnostic criteria. *Neurology*. 1998;51(6):1546-1554.

19. Braak H, Alafuzoff I, Arzberger T, Kretzschmar H, Del Tredici K. Staging of Alzheimer disease-associated neurofibrillary pathology using paraffin sections and immunocytochemistry. *Acta Neuropathol*. 2006;112(4):389-404.

20. Simón-Sánchez J, Dopper EG, Cohn-Hokke PE, et al. The clinical and pathological phenotype of C9ORF72 hexanucleotide repeat expansions. *Brain*. 2012;135(pt 3):723-735.

21. Murray ME, DeJesus-Hernandez M, Rutherford NJ, et al. Clinical and neuropathologic heterogeneity of c9FTD/ALS associated with hexanucleotide repeat expansion in C9ORF72. *Acta Neuropathol*. 2011;122(6):673-690.

22. Konno T, Shiga A, Tsujino A, et al. Japanese amyotrophic lateral sclerosis patients with GGGGCC hexanucleotide repeat expansion in C9ORF72. *J Neurol Neurosurg Psychiatry*. 2013;84(4):398-401.

23. Brettschneider J, Van Deerlin VM, Robinson JL, et al. Pattern of ubiquilin pathology in ALS and FTLD indicates presence of C9ORF72 hexanucleotide expansion. *Acta Neuropathol*. 2012;123(6):825-839.

24. Pringle CE, Hudson AJ, Munoz DG, Kiernan JA, Brown WF, Ebers GC. Primary lateral sclerosis. Clinical features, neuropathology and diagnostic criteria. *Brain*. 1992;115(pt 2):495-520.

25. Morrison BM, Janssen WG, Gordon JW, Morrison JH. Time course of neuropathology in the spinal cord of G86R superoxide dismutase transgenic mice. *J Comp Neurol*. 1998;391(1):64-77.

26. Baker M, Mackenzie IR, Pickering-Brown SM, et al. Mutations in progranulin cause tau-negative frontotemporal dementia linked to chromosome 17. *Nature*. 2006;442(7105):916-919.

27. Yokota O, Tsuchiya K, Arai T, et al. Clinicopathological characterization of Pick's disease versus frontotemporal lobar degeneration with ubiquitin/TDP-43-positive inclusions. *Acta Neuropathol*. 2009;117(4):429-444.

28. Standring S, ed. *Gray's Anatomy: The Anatomical Basis of Clinical Practice*. 39th edition. London, England: Churchill Livingstone; 2004.

29. Josephs KA, Knopman DS, Whitwell JL, et al. Survival in two variants of tau-negative frontotemporal lobar degeneration: FTLD-U vs FTLD-MND. *Neurology*. 2005;65(4):645-647.

30. Hodges JR, Davies R, Xuereb J, Kril J, Halliday G. Survival in frontotemporal dementia. *Neurology*. 2003;61(3):349-354.

- 155 -